Friday, March 18, 2005
MARS: FROM HYDROGEN TO ICE AND IMPLICATIONS FOR CLIMATE CHANGE
8:30 a.m. Salon B

Chairs: J. L. Fastook
J. S. Levy

8:30 a.m. Feldman W. C. * Prettyman T. H. Maurice S. Elphic R. C. Funsten H. O. Gasnault O. Lawrence D. J. Murphy J. R. Nelli S. Tokar R. L. Vaniman D. T.
Topographic Control of Hydrogen Deposits at Mid- to Low Latitudes of Mars **[#1328]**
A close study of the correspondence between relative maxima in water-equivalent hydrogen abundances with relative maxima in the topography at mid- to low latitudes of Mars suggest that weather patterns control the deposition onto, and/or vapor diffusion into surface soils from the atmosphere.

8:45 a.m. Murray J. B. * Muller J.-P. Neukum G. Werner S. C. Hauber E. Markiewicz W. J. Head J. W. III Foing B. H. Page D. Mitchell K. L. Portyankina G. HRSC Investigator Team
Evidence from HRSC Mars Express for a Frozen Sea Close to Mars' Equator **[#1741]**
We present evidence for a presently-existing frozen sea, with surface pack-ice, at 5°N, 150°E, age ca. 5 million years. It measures ca. 800 × 900 km and averages ca. 45 m deep. It has probably been protected from complete sublimation by ash and a sublimation lag of exposed sediment.

9:00 a.m. McBride S. A. * Allen C. C. Bell M. S.
Prospecting for Martian Ice **[#1090]**
Relations between craters and ice-wedge polygons were examined on MGS images to constrain the thickness and age of a possible ice-rich mantle in the northern mid-latitudes. Results indicate the mantle is about 40 m thick and dates from before 5 Ma.

9:15 a.m. Fishbaugh K. E. * Hvidberg C. S.
Effect of Flow on the Internal Structure of the Martian North Polar Layered Deposits **[#1331]**
We investigate the effect of flow on the internal layer structure of the cap and compare the results to the actual structure observed in image data. The results have implications for interpretation of the climate record preserved in the layers.

9:30 a.m. Marchant D. R. * Head J. W. III
Equilibrium Landforms in the Dry Valleys of Antarctica: Implications for Landscape Evolution and Climate Change on Mars **[#1421]**
An understanding of the origin and evolution of equilibrium landforms in the Antarctic Dry Valleys may be helpful in elucidating the origin of some enigmatic landforms on Mars and in interpreting recent changes in the Martian climate.

9:45 a.m. Levy J. S. * Head J. W. III Marchant D. R. Kreslavsky M. A.
Evidence for Remnants of Late Hesperian Ice-rich Deposits in the Mangala Valles Outflow Channel **[#1329]**
We assess several possible origins for a smooth unit on the floor of Mangala Valles, interpreting it as an ice-rich remnant created by ponding and ice-cover deflation during the waning stages of the outflow channel flood emplacement.

10:00 a.m. Head J. W. III* Marchant D. R. Agnew M. C. Fassett C. I. Kreslavsky M. A.
Regional Mid-Latitude Late Amazonian Valley Glaciers on Mars: Origin of Lineated Valley Fill and Implications for Recent Climate Change **[#1208]**
Evidence is presented that lineated valley fill in the Deuteronilus mid-latitude region of Mars originated from snow and ice accumulation and glacial flow during periods of high obliquity in the Amazonian.

10:15 a.m. Helbert J. * Benkhoff J.
Beyond the Equilibrium Paradigm — Glacial Deposits in the Equatorial Regions of Mars **[#1352]**
We will show, that even in the equatorial regions of Mars ground ice deposits can be stable over long periods of time. The main assumption we have to do is, that the near surface layer of Mars is not in an equilibrium state.

10:30 a.m. Elphic R. C. * Feldman W. C. Prettyman T. H. Tokar R. L. Lawrence D. J.
Head J. W. III Maurice S.
Mars Odyssey Neutron Spectrometer Water-Equivalent Hydrogen: Comparison with Glacial Landforms on Tharsis **[#1805]**
Mars Odyssey neutron spectrometer measurements indicate enhanced water-equivalent hydrogen abundances on the western slopes of the Tharsis Montes, possibly in association with relict buried ice.

10:45 a.m. Fastook J. L. * Head J. W. III Marchant D. R. Shean D. E.
Ice Sheet Modeling: Mass Balance Relationships for Map-Plane Ice Sheet Reconstruction: Application to Tharsis Montes Glaciation **[#1212]**
We apply the properties of the Mars atmosphere to models of mass balance and spatial distribution on the flanks of Tharsis Montes; these lead to patterns that are strikingly similar to the geological evidence for ice accumulation and glacial flow.

11:00 a.m. Ishii T. * Miyamoto H. Sasaki S.
Viscous Flows from Poleward-facing Walls of Impact Craters in Middle Latitudes of the Alba Patera Area **[#2172]**
Inclinations of poleward-facing crater walls are smaller than those of equatorward-facing walls in middle latitudes of the Alba Patera area, which suggests that viscous flows of ice-rich materials would occur preferentially on poleward-facing slopes.

11:15 a.m. Shean D. E. * Head J. W. III Marchant D. R.
Debris-covered Glaciers Within the Arsia Mons Fan-shaped Deposit: Implications for Glaciation, Deglaciation and the Origin of Lineated Valley Fill **[#1339]**
We interpret flow-like features at Arsia Mons as debris-covered glaciers representing the most recent phases of glaciation in this region, providing insight into processes of glaciation and deglaciation on Mars. We discuss applications to other areas containing candidate glacial deposits.

11:30 a.m. Sakimoto S. E. H. *
Central Mounds in Martian Impact Craters: Assessment as Possible Perennial Permafrost Mounds (Pingos) **[#2099]**
We characterize topography for and model martian polar region impact crater central mounds as potential perennial permafrost mounds (pingos).

Topographic Control of Hydrogen Deposits at Mid- to Low Latitudes of Mars, W.C. Feldman[1], T.H. Prettyman[1], S. Maurice[2], R. Elphic[1], H.O. Funsten[1], O. Gasnault[2], D.J. Lawrence[1], J.R. Murphy[3], S. Nelli[3], R.L. Tokar[1], D.T. Vaniman[1], [1]Los Alamos National Laboratory, Los Alamos, NM, wfeldman@lanl.gov, [2]CESR, Toulouse, Fr., [3]New Mexico State University, Las Cruces, NM.

Introduction: Global surveys of hydrogen deposits on Mars have revealed three major reservoirs [1,2,3,4,5]. The two most abundant reservoirs reside at high latitudes, poleward of about ±60°. Significant reservoirs with minimum abundances between 2% and 10% water-equivalent hydrogen (WEH) reside at mid-to low latitudes. Initial analyses of the lower latitude deposits indicate they are most likely in the form of hydrated minerals [7,8] although deposits of water ice cannot be ruled out if they are covered by dry layers having sufficiently low permeability to effectively isolate them from the atmosphere. Most low latitude reservoirs are hydrogeologically isolated from those at high latitudes because of their relatively high altitudes and/or deep boundary canyons. Their recharge can therefore not occur by connection to the polar caps through a possible global water table [9]. On the other hand, the actual WEH emplacement mechanism is not known because the locations of low- to mid latitude reservoirs correlate poorly with most commonly known measures of WEH stability in the current Martian environment [e.g., local maxima in WEH occur in regions of both high and low albedo (and hence low and high subsurface temperatures, respectively), and high and low relative humidity] [8]. We present evidence here that the topographic control of weather patterns (orographic effects) could account for the observed WEH distribution at low to middle latitudes.

Data Analysis: In this study we compare the abundance of WEH measured using the Mars Odyssey Neutron Spectrometer [2,6], shown in the top panel of Fig. 1, with the topography measured using the Mars Orbiting Laser Altimeter [10]. Overlays of six meridional cuts, shown in the bottom two panels of Fig. 1, are used for this purpose. The longitudes of these cuts are shown by the white vertical lines in the top panel of Fig. 1. Progressing from west to east, we note a single maximum in WEH at –179 E longitude that peaks just north of the sharp topographic boundary that separates the highlands in the south from the lowlands in the north. At –79 E, three relative maxima in WEH are seen. The most northerly at 40 N overlies the relatively high terrain of Tempe Terra. The central maximum overlies the high terrain just north of Valles Marineris (at 5 S) that also forms the northern boundary of Solis Planum. The most southerly maximum (at 35 S) overlies the cordillera ridge that marks the southern boundary of Solis Planum. We note that the WEH content of the northern boundary of Solis Planum is higher than that of the southern boundary, which is to be expected if weather patterns drive WEH deposition from atmospheric water vapor, which maximizes in the north [11]. The next meridional cut at -47E reveals relative maxima in WEH at 30 N, 2 N, and 35 S. Here again, the central maximum occurs at the main north/south topographic boundary of Mars. A small convex-upward inflection in the WEH trace at 15 S also matches the north-facing side of Valles Marineris at 20 S. The next three meridional cuts at +15 E (Arabia Terra), +67 E (Syrtis Major Planum), and +85 E (Tyrhena Terra) also show relative maxima or convex upward inflections in WEH that closely correspond to relative maxima or convex-upward inflections in the topography.

Conclusions: A close study of the correspondence between relative maxima in WEH abundances with relative maxima in the topography at mid- to low latitudes of Mars suggest that weather patterns control the deposition onto, and/or vapor diffusion into surface soils from the atmosphere. The general concentration of atmospheric water vapor is observed to occur north of the equator [11]. Although water ice is nowhere stable equatorward of ± 45° [8], making it less likely that observed WEH abundances result from weather-related water ice deposits, many different hydratable minerals are stable throughout this region, [12,13,14] and are sensitive to weather factors, particularly RH. Quantitative calculations using potential hydrous minerals show that no one mineral family can explain all WEH observations at low- to mid latitudes of Mars, suggesting the need for a heterogeneous mixture of hydratable minerals [8,14].

References: [1] Feldman et al., Science, 281, 1496-1500, 2002; [2] Feldman, W.C., et al., JGR, 109, doi:10.1029/2003JE002160,2004a; [3] Boynton et al., Science, 297, 81-85, 2002; [4] Mitrofanov, I., et al., Science, 297, 78-81, 2002; [5] Tokar, R.L. et al.,, GRL, 29, doi:/10.1029/2002GL015691,2002; [6] Prettyman, T.H., et al., JGR, 109, doi:10.1029/2003JE02139,2004; [7] Basilevsky, A.T., et al., Solar System Res., 37, 387-396, 2003; [8] Feldman, W.C., et al., GRL, 31, doi:10.1029/2004GL020181,2004b; [9] Feldman, W.C., et al., GRL 31, doi:10.1029/2004GL020661, 2004c; [10] Smith,D.E., et al., Science, 284 1495-1507, 1999; [11] Smith, M.D., JGR, 107, doi:10.1029/2001JE001522,2002; [12] Bish, D.L., et al., Icarus, 164, 96-103, 2003; [13]

Möhlmann, D.T.F., Icarus, 168, 318-323, 2004; [14] Fialips et al., Icarus, submitted, 2004.

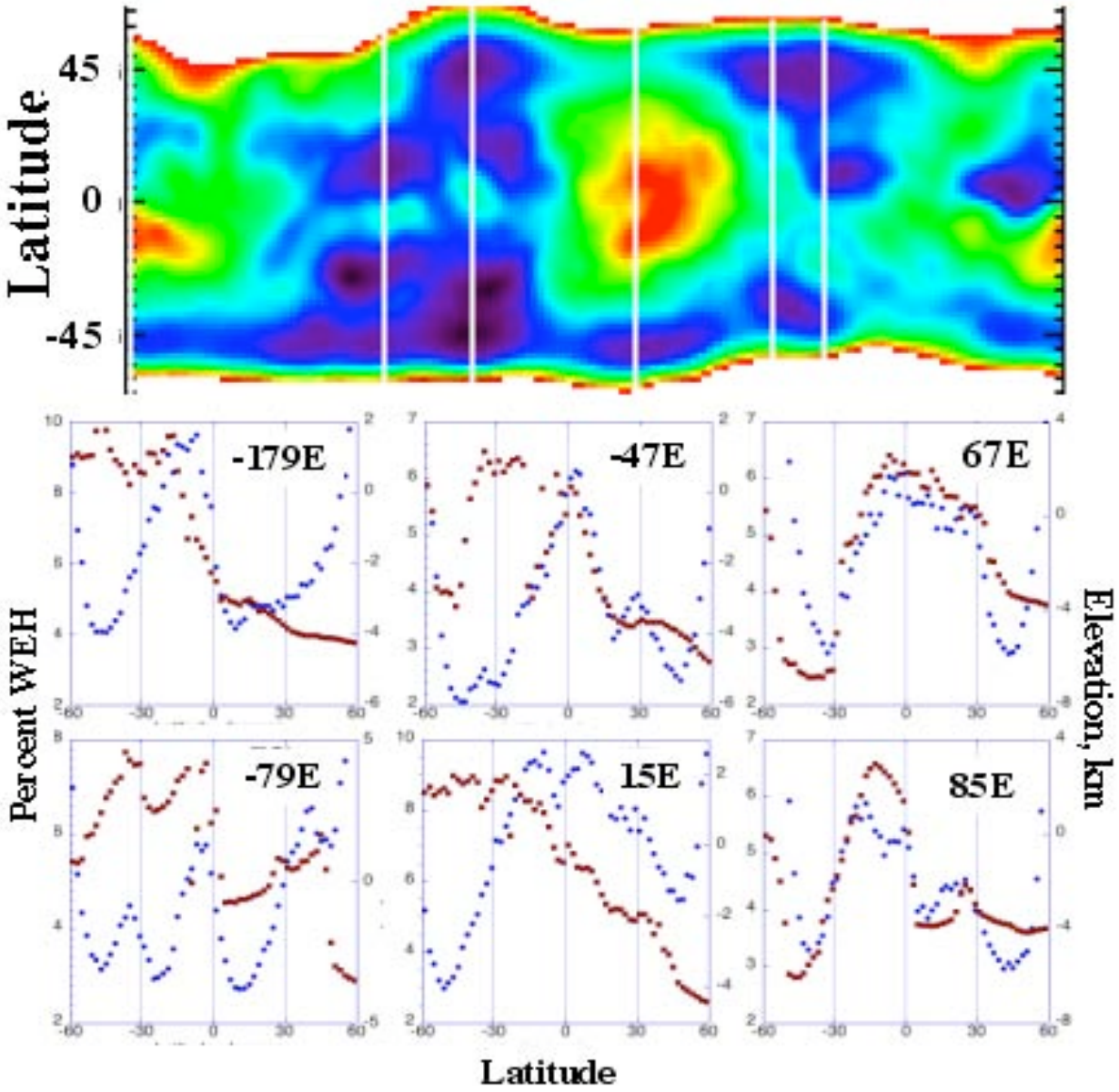

Figure 1: Map of the distribution of Water-Equivalent Hydrogen (WEH) between 2% (deep purple) and 10% (red) by mass is given in the top panel. The six white lines give the longitudes of meridional cuts through the WEH abundances (blue symbols, scale at left-hand margin) and the topography (red symbols, scale at right-hand margin) shown in the two bottom panels.

EMBARGOED BY NATURE MAGAZINE UNTIL MID MARCH

EVIDENCE FROM HRSC MARS EXPRESS FOR A FROZEN SEA CLOSE TO MARS' EQUATOR.
John B. Murray[1], Jan-Peter Muller[2], Gerhard Neukum[3], Stephanie C. Werner[3], Ernst Hauber[4], Wojciech J. Markiewicz[5], James W. Head III[6], Bernard H. Foing[7], David Page[1,8], Karl L. Mitchell[9], Ganna Portyankina[5] & the HRSC Co-Investigator Team. [1]Dept. of Earth Sciences, The Open University, Milton Keynes MK7 6AA, U.K. j.b.murray@open.ac.uk [2] Dept. of Geomatic Engineering, University College London, Gower St., London WC1E 6BT, U.K. [3] Geosciences Institute, Freie Universität Berlin, Malteserstr. 74-100, Building D, 12249 Berlin, Germany. [4] DLR-Institut für Planetenforschung, Rutherfordstrasse 2, D-12489 Berlin-Adlershof, Germany. [5] Max Planck Institute for Aeronomy, Max-Plank-Str. 2, 37191 Katlenburg-Lindau, Germany. [6] Dept. of Geological Sciences, Brown University, Box 1846, Providence, Rhode Island 02912, U.S.A. [7] Chief Scientist, ESA Research & Scientific Support Dept., ESTEC/SCI-SR postbus 299, 2200 AG Noordwijk, The Netherlands. [8] Dept. of Mineralogy, The Natural History Museum, London SW7 5PB, U.K. [9] Environmental Science Dept., Lancaster University, Bailrigg, Lancaster LA1 4YQ, U.K.

Introduction: The Cerberus Fossae fissures on Mars are the source of both lava and water floods [1] dated at between 2 &10 million years old. Evidence for resulting lava plains has been identified in eastern Elysium, but seas and lakes from these fissures and previous flooding events were presumed to have evaporated and sublimed away [2]. HRSC images from the ESA Mars Express spacecraft indicate that they may still be there. We have found evidence consistent with a presently-existing frozen body of water, with surface pack-ice, around +5º latitude and 150º east longitude in southern Elysium. It measures about 800 km x 900 km and averages up to 45 m deep: similar in size and depth to the North Sea. It has probably been protected from complete sublimation by a surface sublimation lag formed from suspended sediment exposed by early loss of the surface ice. Its age from crater counts is 5 ±2 Ma.

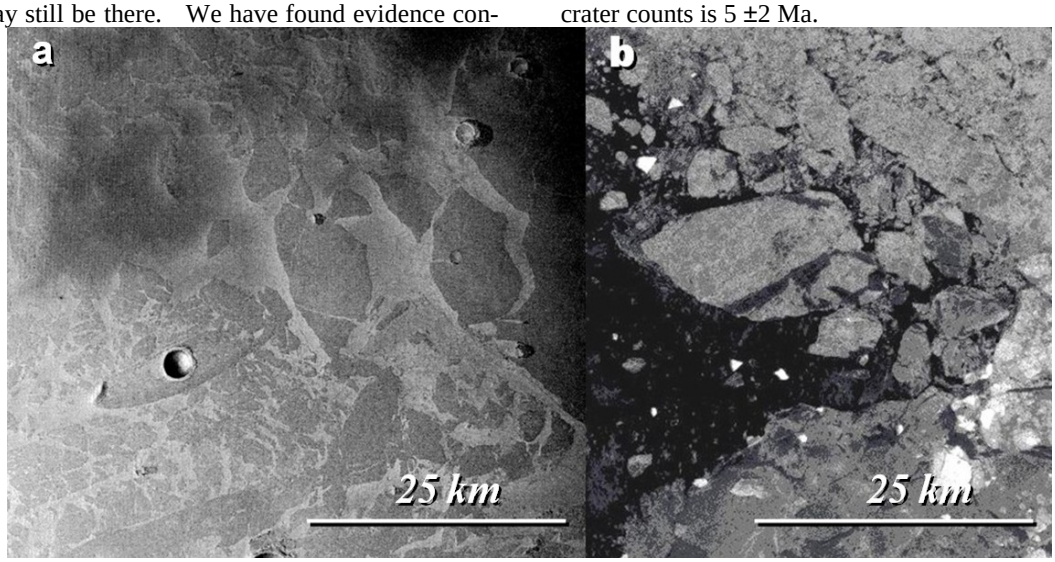

Fig 1. (left) shows extensive fields of large fractured platy features on a horizontal surface, visible near the south end of an HRSC image taken on 2004 Jan. 19, compared with pack-ice in the Antarctic (right). Individual plates are of all sizes from 30 m up to >30 km, with clear signs of break-up, rotation and horizontal drift for distances of several km. The plates show characteristic differences from platy features elsewhere on Mars and in the east of Elysium Planitia. The latter have been interpreted to be rafts of solidified lava floating on the surface of large flood basalts [3], but several observations indicate that this cannot be the case in this area.

Crater-count ages: Surface ages were determined from the size-frequency distribution [4] of 66 impact craters on HRSC images, which suggest a resurfacing event about 5 Ma ago. Counts of 268 craters on MOC images show that the plates are older than the brighter inter-plate areas, by about 1 Ma. Basalt lava flows of 50m depth can remain partially molten at the centre for only about 5 years, so these plates cannot be the result of surges of lava carrying previously solidified crust.

Flood characteristics: A drop in surface level has occurred after flooding of 18 to 85 m (equivalent to about 9% to 16% of the depth prior to flooding) within flooded impact craters (fig. 2). Ponded lava cannot

seep into sediments, evaporate or sublime, & thermal contraction would amount to less than 1%.

Where the plates have encountered craters and islands, these have acted in a similar manner to ice-breakers as the plates drifted past them, leaving straight or curved leads downstream of uniform width (L, fig. 2). These are not found within lava rafts. These lanes are still very smooth at the 10 metre scale, as are similar features in pack-ice on Earth. Also, the plates attain sizes one to two orders of magnitude greater than the largest known terrestrial basalt rafts. Both these observations, together with the very horizontal surface (<5 m height variation over more than 60 km, i.e.<0º.005, corresponding to terrestrial tidal sea surface slopes in some estuarine situations) imply an extremely mobile fluid, with similar characteristics to water.

Other characteristics also resemble pack-ice.

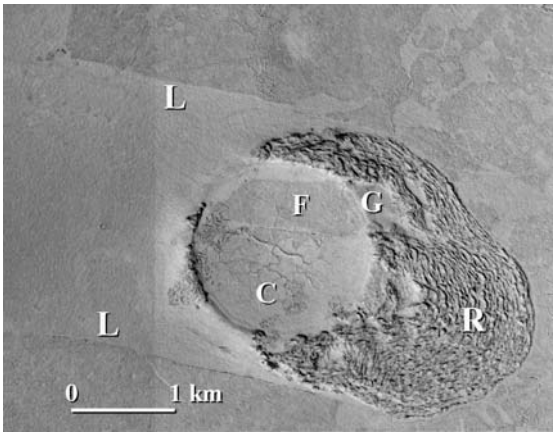

Fig. 2 is a MOC image showing pressure ridges R with wavelengths between 10 and 70 m within the rubble pile on the upstream side (right). Caused by plate drift, these appear to have extended outward from the crater edge as the liquid level dropped and the frozen surface was grounded progressively further down the outer slopes of the crater. They are strikingly similar to rubble piles of sea ice that form around islands in the Arctic and Antarctic. The sagging and consequent surface cracking **C** within the crater itself as the level dropped are also visible. One plate **F** has drifted into the crater when the level was higher through the gap in the rim **G**, but then become grounded in its present position as the surface lowered, draping it over the NE rim.

Pack-ice: We interpret the structures and textures to be due to pack-ice formed as a moving and fracturing thermal boundary layer on top of ponded aqueous floodwater which later froze. Reasonable estimates of the depth can be made by using the rim height to diameter ratios of partially submerged impact craters, assuming these are fresh. 14 crater rims have been identified from their traces partially above or just below the ice, yielding initial water depths of between 31 and 53 m, with an average at 45 m. MOLA profiles across three flooded craters indicate that low parts of the rim are still 0 to 30 m above the mean ice level, suggesting that evaporation, sublimation and seepage sagging may have lowered the ice thickness to a present mean value of around 30 m ice depth.

Ice is unstable at the surface of Mars at the present time due to sublimation in the 6 mbar atmosphere, but it is thought that huge volumes of volcanic ash were also erupted from Cerberus Fossae [3] which if contemporaneous with water emission would have formed a substantial protective layer on the ice. Depending on the porosity and thermal properties of this layer, the subsequent lowering of the floe surfaces could be very slow. Subliming water vapour migrating through the pores will over time help to sinter and chemically bind the particles to form a stronger sublimation lag.

We suggest the following sequence of events: firstly, pack-ice formation with a volcanic ash covering, secondly, remobilisation, break-up and drift of pack-ice, and cessation of volcanic activity, thirdly, freezing of entire body of water, and finally, the sublimation of the unprotected ice between the ash-covered ice-floes, gradually exposing the suspended sediment at the surface to form a protective layer with a younger age than the floes.

The question remains as to whether the frozen body of water is still there, or whether the visible floes are preserved in a sublimation residue draped over the substrate. Two observations suggest that it is still there:

1. Submerged craters are too shallow, suggesting that most of the ice is still within the craters.

2. The surface is too horizontal. Ice depth estimates above indicate that the “sea bottom” varies in altitude by 55 m. Had the ice been lost, this should have resulted in greater height variation.

Micro-organisms found within deep-sea hydrothermal vent communities are common ancestors to many forms of life on Earth, and a Martian aquifer having intermittent contact with the surface might provide an opportunity not only for troglodytic life to develop, but to be disgorged on to the surface, and the frozen sea described here would be a prime candidate area for the preservation and discovery of its remains.

References: [1] Berman, D. C. & Hartmann, W. K. (2002). *Icarus 159*, 1-17. [2] Carr, M.H. & Head III, J.W. (2003). *JGR 108*, No. E5, 5042. [3] Keszthelyi, L., McEwen, A.S. & Thordarson, T. J. (2000) *JGR 105*, E6, 15,027-15,049. [4] Hartmann, W.K. & Neukum, G. (2001). *Space Sci. Rev. 96*, 165-194.

Prospecting for Martian Ice. S.A. McBride[1], C.C. Allen[2], M.S. Bell[3], [1]Cornell University, Ithaca, NY, [2]NASA Johnson Space Center, Houston, TX, [3]Lockheed Martin @ Johnson Space Center, Houston, TX.

Introduction: During high Martian obliquity, ice is stable to lower latitudes [1,2] than predicted by models of present conditions and observed by the Gamma Ray Spectrometer (~60°N) [3]. An ice-rich layer deposited at mid-latitudes could persist to the present day; ablation of the top 1 m of ice leaving a thin insulating cover could account for lack of its detection by GRS. The presence of an ice-layer in the mid-latitudes is suggested by a network of polygons, interpreted as ice-wedge cracks [4,5]. This study focuses on an exceptional concentration of polygons in Western Utopia (section of Casius quadrangle, roughly 40°-50°N, 255°-300°W) [6]. We attempt to determine the thickness and age of this ice layer through crater-polygons relations.

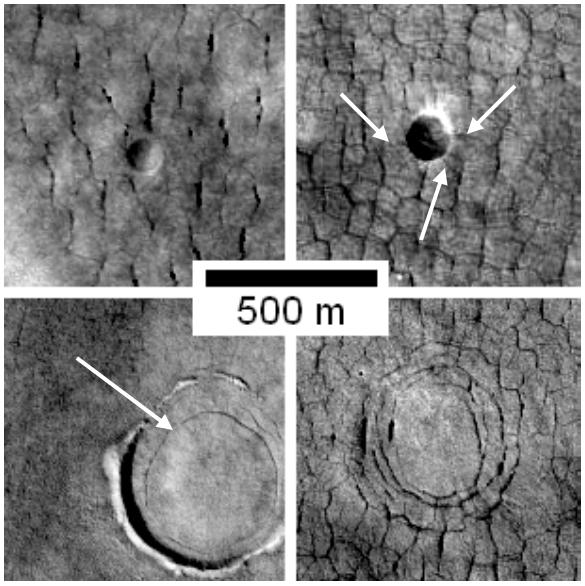

Figure 1 – Crater morphologies in relation to polygonal fractures as seen in MOC images (clockwise from top left): fresh (image R0301150); radial cracks (M0401631); concentric cracks (R0502250); inner wall cracks (R0501314).

Methods: Using a list of MOC frames showing polygons [7], we completed a survey of craters within 9120 km^2 of polygonal terrain in all narrow angle MOC images in the latitudes 30°-65°N released between 09/97 and 09/03 [8]. 72% of these polygons were in the Casius quadrangle. For craters with diameters greater than 100 m we recorded location, diameter, and crater morphology (Figure 1): fresh, radial cracks, concentric cracks, or inner wall cracks. Fresh craters appear younger than polygons as they are not cross-cut by any cracks. Radial cracks around a crater are interpreted as cracks forming in relation to the free face of the inner crater wall. Concentric cracks are circular rings of cracks in an otherwise normal polygonal network. Inner wall cracks are similar to concentric except they form in craters with rims still protruding. The presence or absence of thermokarst features and the density of craters smaller than 100 m were also noted.

Thickness of the ice layer: Many craters are only visible as concentric cracks in an otherwise random polygon network. The pattern of ice-wedge cracking appears to be controlled by an underlying crater rim or fractures associated with cratering. There appears to be a diameter dependent boundary between such concentric cracks, and inner wall cracks forming around a still-protruding rim. Apparently craters up to a certain size have been buried by the ice rich layer, while larger craters have not. The largest buried crater has a diameter of 1.12 km, while the smallest partially buried crater with a protruding rim has a diameter of 0.46 km. The diameter of the smallest craters with protruding rims shows a slight increase with latitude (Figure 2).

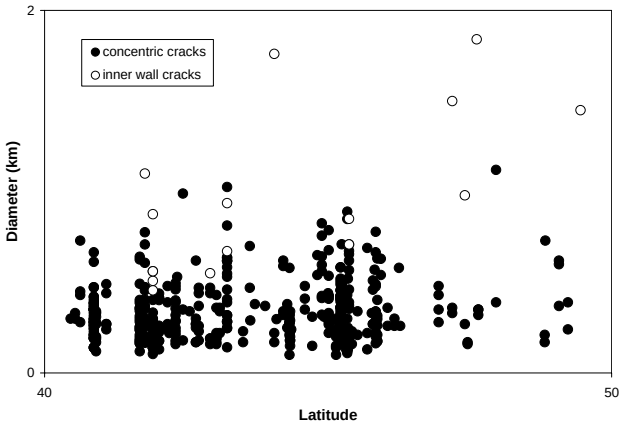

Figure 2 – Crater morphology by size and latitude showing diameter-dependent transition.

A sharp decline in the density of very small craters (< 100 m) northwards suggests they are being degraded or buried. Mantling has been suggested to have recently operated in the northern plains [1,9]. The diameter dependent morphology transition of craters supports this hypothesis, and provides a method of gauging the thickness of the mantle. As the crater may be a preferred site of deposition of ice and dust, the rim height rather than the depth is a better parameter to use for crater burial. Using the relation $h_{rim}=0.04D^{0.31}$ [10], the mantling ice is

calculated to be 31 to 41 m thick. As this expression for rim height is for all Martian craters, including partially buried ones, the calculated thickness represents a minimum value.

Age of the ice layer: 97% of craters observed in the Casius quadrangle predate polygon formation, suggesting a very young age for the ice. By adjusting the calibrated lunar crater flux for Martian gravity, orbit, and atmosphere, others have developed an absolute dating system for Mars. According to these crater density isochrons (Figure 3) [11], polygons were forming until between 0.5 and 10 Ma.

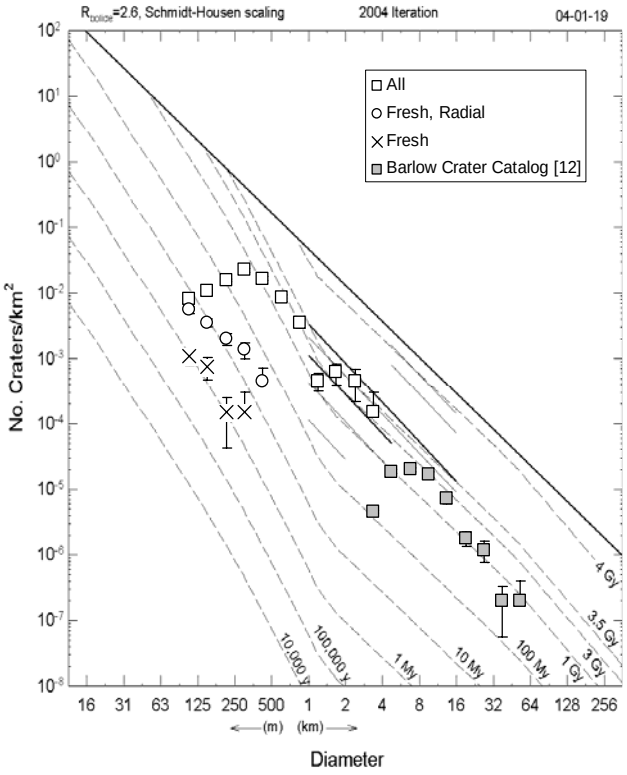

Figure 3 – Density distribution for craters associated with polygons in the Casius quadrangle, as well as all craters > 3 km [12]. Isochrons from [11].

Fresh and radially cracked crater abundances suggest that the mantling unit stopped forming at 5 to 50 Ma, older than the last high obliquity cycle. Mars has greater fluctuations of obliquity than the Earth, including regular oscillations as well as a generally higher level of obliquity before 5 Ma [13,14]. Isochrons [11] suggest the formation of the majority of the blanket before the drop to present obliquity ranges at 5 Ma, as in [2,14]. Perhaps mantling occurs in the high amplitude part of the obliquity oscillations, and was magnified before 5 Ma.

All craters, including those seen only as concentric rings of polygons, align well with a count done for larger craters (D = 3-80 km) [12] that gave a Hesperian-Amazonian age. However, densities decrease for craters smaller than 1 km, again suggesting a mantle burying craters up to this size.

Nature of the ice layer: The survey also revealed some related trends in ice-associated features. Most polygons north of 60°N are light relative to their surroundings, while most south of 60°N are dark. Thermokarst in the polygons is present mostly between 40°-50°N, mostly in the northern half of this range. Indicators of climate change include widening polygons, polygons on thermokarst, mantled thermokarst, and layered thermokarst scarps.

The polygons scattered across the rest of the northern plains differ considerably from the Casius concentration. The northern polygons are in general wider and less well defined. On average the crater distribution matches the Casius quadrangle; however, some areas have the appearance of being much older due to extensive cratering. The global diameter dependent transition from concentric to inner wall cracks matches well with the Casius quadrangle.

Conclusion: An ice rich layer approximately 40 m thick is revealed by the presence of recently active ice-wedge polygons in at least part of the Casius quadrangle, and possibly more extensively across the northern plains. Higher obliquity probably caused deposition of the mantle before 5 Ma; formation of polygons has continued until the present.

Acknowledgements: Lisa Kanner for her list of MOC images containing polygons; Nadine Barlow for her crater catalog of the Casius quadrangle; and Susan Sakimoto for guidance on crater morphology.

References: [1] Head J.W. et al. (2003) *Nature*, 426, 797-801. [2] Kreslavsky M.A. and Head J.W. (2004) *LPSC XXXV*, Abstract #1201. [3] Boynton W.V. et al. (2002) *Science*, 297, 81-85. [4] Seibert N.M. and Kargel J.S. (2001) *Geo. Res. Lett.*, 28, 899-902. [5] Mellon M.T. (1999) *LPSC XXX*, Abstract #1118. [6] Kanner L.C. et al. (2004) *LPSC XXXV*, Abstract #1982. [7] Kanner L.C. (2004) *personal contact*. [8] Malin M.C. et al. (1997-2003) *Malin Space Center Systems Mars Orbiter Camera Image Gallery* (www.msss.com/moc_gallery). [9] Kostama V.P. et al. (2004) *LPSC XXXV*, Abstract #1203. [10] Garvin J.B. et al. (2003) *SICM*, Abstract #3277. [11] Hartmann W.K. et al. (2002) *Planetary Science Institute* (www.psi.edu/projects/mgs/isochron.html). [12] Barlow N.G. (2004) *personal communication*. [13] Laskar J. et al. (2004) *LPSC XXXV*, Abstract #1600. [14] Manning C.V. et al. (2004) *LPSC XXXV*, Abstract #1818.

EFFECT OF FLOW ON THE INTERNAL STRUCTURE OF THE MARTIAN NORTH POLAR LAYERED DEPOSITS. K. E. Fishbaugh[1] and C. S. Hvidberg[2], [1]International Space Science Institute, Hallerstrasse 6, Bern, Switzerland CH 3012, fishbaugh@issi.unibe.ch; [2]Niels Bohr Institute, University of Copenhagen, Juliane Maries Vej 30, Copenhagen, Denmark DK 2100, ch@gfy.ku.dk.

Introduction: The varying deposition rates of ice and particulates reflected in the alternating bright and dark layering of the martian polar layered deposits (PLD) has sparked an interest in correlating the PLD layering with changes in orbital parameters such as obliquity [e.g.,1, 2, 3]. If this correlation exists, the polar layers may be an invaluable record of Mars' recent climate history as changes in orbital parameters are major regulators of climate. In order to attach particular layers or layer sequences to particular changes in orbital parameters, one must assume that the stratigraphic sequence has been preserved and that a timescale can be reconstructed.

If the layers are subject to flow, the stratigraphy can be affected in several ways. As pointed out by Clifford et al. [3], flow can stretch and thin layers, the amount increasing with depth in the ice. This process leaves intact the climate record possibly recorded in the PLD, but the timescale needs to be adjusted (e.g., with flow models that assume a certain deposition rate and take the layer thinning into account). In some cases, ice flow may disturb the stratigraphic record. For example, large scale flow can create disconformities, and localized flow instabilities can lead to folding and boudinage.

The goal of this study is to determine what effects flow might have on the internal layer structure of the north polar cap and whether these effects are observed in the data.

Initial Assumptions. We begin the flow modeling by assuming an initial layer structure and then allowing it to flow, using two different mass balance scenarios. We term the initial layer structure a "Layer Cake". Each layer is initially flat and of equal thickness. This scenario involves the least complicated assumptions about the unknown mass balance (deposition and ablation) history of the cap. Additionally, the PLD are deposited relatively quickly on a geologic timescale so that flow is assumed not to have affected the ice sheet to an appreciable degree until after most of it was deposited. If the cap has been flowing (at an appreciable rate) throughout its history, the situation involves many more parameters whose values are unknown. We do not attempt to model how troughs are formed, though, as explained below, we assume the presence of troughs (through their effect on the mass balance) in one of our model runs. It is also assumed that throughout the time during which the cap has been flowing, the mass balance has not changed.

Flow modeling: The flow model is a simple isothermal, two-dimensional, time-varying, numerical model. The model assumes that ice deforms according to a power law (Glen's flow law) simplified to shear stresses only, and solves the mass conservation equation. The model assumes a mass balance (deposition and sublimation pattern) and allows the ice cap to evolve over time. Model outputs are surface evolution, internal layer structure, and particle trajectories of ice particles deposited at the surface. We run the model on a Layer Cake ice cap with two example mass balance patterns.

Model 1: No deposition or sublimation. The Layer Cake flows but no further deposition or ablation has occurred since the layers were deposited. This serves as an end-member example and is only an approximation of reality if the shapes of the cap and its layers have been affected more by flow than by mass balance since their deposition. The purpose of this model is to isolate the effect of flow on the layer structure.

Model 2: Fisher Accublation. The Layer Cake flows, and its mass balance is described by Fisher Accublation [4] in which deposition occurs on the flats areas between polar troughs and ablation occurs within the troughs. This could most accurately describe the current mass balance of the northern cap. The purpose of this model is to study the combined effect of flow and deposition/sublimation associated with polar troughs. Note that the troughs remain in a fixed position in this model.

The flow models can be improved by considering more complicated initial layer structures and by adding the effects of changing obliquity on temperatures and hence on flow rates.

Layer Correlation and Determination of Structure: We compare the layer structure predicted by the flow models to observations of the actual layers using image (primarily MOC) and MOLA data. For our preliminary analysis of layer structure visible in MOC images, we choose example PLD outcrops based on the following criteria: 1) images identified by [5] as containing their "marker bed" and 2) images of layered deposit outcrops containing other conspicuous layers which could possibly be used as markers; we will term the latter layers "reference layers" so as not to confuse them with the "marker

bed" of [5]. The correlations of particular reference layers from one location to another are performed based on morphology. While the morphology can change from one location to the next, in most cases, a distinct layer remains distinct, regardless of its small-scale surface texture. Additionally, the pattern of layering surrounding a reference layer (e.g., a package of thin layers above) can also be used to identify it.

The chosen example images have been registered to a MOLA DEM (res.≈120m/pix) by S. Byrne as described in [6] and have errors in their positions of about 10–100m [7]. For our study we are interested in the overall large scale structure of the layering, thus the inaccuracies are relatively insignificant. In the example images, we have located reference layers and the marker bed, and we have derived elevations of those layers from the co-registered MOLA data.

Figure 1 shows preliminary results of the layer correlation. It is evident that the upper layers curve while the lower layers are flatter and appear more like the Layer Cake. Previous flow modeling has shown that when one begins with a Layer Cake ice sheet and allows it to flow, the upper layers will follow the surface of the ice sheet (and so will curve) while the lower layers will follow the base [4]. However, if an ablation zone is present near the ice sheet margin, flow can bring deep layers to shallower depths near the margin and can thicken them as well, a possibility for which we will search in the MOC data.

We plan to perform more layer correlations in more areas of the cap (including THEMIS images), to search for possible unconformities, and to investigate layer thinning with depth. These analyses will help us to better understand the internal stratigraphy of the north polar cap and to better compare it to the layering pattern predicted by flow models. Additionally, we plan to improve the accuracy of our reference layer elevation measurements by better registering image data to the MOLA DEMs.

Comparison with Previous Studies: Using Fourier Analysis of layer packages and matching analyses similar to those used for deep sea cores, Milkovich and Head [8] find that the layers within the northern PLD are curving. Those results are consistent with the upper layer structure in our layer correlation analysis and in previous flow models [e.g., 4].

Byrne and Ivanov [7] also predict this structure for at least the upper layers of the southern PLD and suggest that the layers were initially deposited on a mound. Due to the shape of the layer structure they constructed and comparison with theoretical shapes formed by a flowing ice cap, the authors also suggest that flow may not have been as important in determining cap shape in the south as has mass balance (unless the mass balance is distributed non-uniformly or the flow properties vary within the cap). Indeed, the shapes, ages [9], and geologic histories [10, 11] of the two caps are dissimilar so that one could also expect their flow histories to be dissimilar.

Our analyses can be useful for studies involving interpretation of the climate record within the polar layered deposits and for interpretation of MARSIS radar data of the caps.

Acknowledgements: This study is partially funded by a grant to K.E.F. from the American Scandinavian Foundation. Thanks are extended to Shane Byrne (MIT) for providing data for use in GIS software.

References: [1] Cutts, J. and B. Lewis (1982) *Icarus 50*, 216-244. [2] Laskar et al. (2002), *Nature 419*, 374-377. [3] Clifford et al. (2000), *Icarus 144*, 210-242. [4] Fisher, D. (2000), *Icarus 144*, 289-294. [5] Malin, M. and K. Edgett. (2001), *JGR 106 (E10)*, 23429-23570. [6] Byrne, S. and B. Murray (2002), *JGR 107 (E6)*. [7] Byrne, S. and A. Ivanov (2004), *JGR 109 (E11)*. [8] Milkovich, S. and J. Head (2005) *JGR, in press*. [9] Herkenhoff, K. and J. Plaut (2000), *Icarus 144*, 243-253. [10] Fishbaugh, K. and J. Head (2001), *Icarus 154*, 145-161. [11] Kolb, E. and K. Tanaka (2001), *Icarus 154*, 22-39.

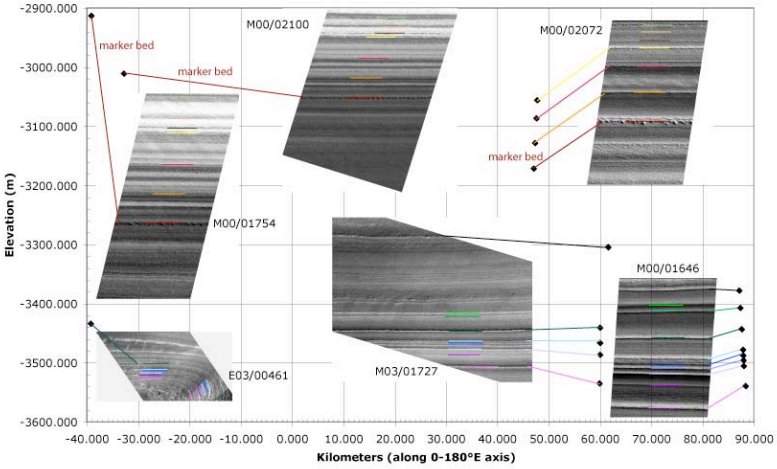

Figure 1. Layer correlations. Red "marker bed" refers to that defined by [5]. Other colors delineate other reference layers. Black dots indicate elevations of some example reference layers. Note that these preliminary results are presented in absolute elevation of the layers rather than depth from the surface of the ice cap, so that no information on the correlation between layer structure and ice cap surface shape is illustrated here. In the future, results will be presented in both formats.

EQUILIBRIUM LANDFORMS IN THE DRY VALLEYS OF ANTARCTICA: IMPLICATIONS FOR LANDSCAPE EVOLUTION AND CLIMATE CHANGE ON MARS: David R. Marchant[1] and James W. Head. [1]Department of Earth Sciences, Boston University, Boston MA 02215 (marchant@bu.edu.) [2]Department of Geological Sciences, Brown University, Providence, RI 02912

Introduction: The very low atmospheric temperatures and limited availability of liquid water in parts of the Antarctic Dry Valleys (ADV) makes them compelling analogs for current martian environments. Although classified as a single, hyper-arid, cold-polar desert, the ADV region is more appropriately divided into a series of narrow climatological zones. Each zone fosters a unique suite of equilibrium landforms [1]; in this context, equilibrium landforms are those unconsolidated features produced solely by geomorphic processes operating within a given microclimate zone. Of course some landforms in the ADV evolved over a range of climatic conditions, but many formed from processes operating at uniform rates and under non-changing climate conditions [1]. In this tectonically stable region then, evidence for partial dissection and/or unstable modification of equilibrium landforms may suggest variation in geomorphic processes brought on by interval(s) of climate change. Our study of the origin, evolution, and temporal migration of equilibrium landforms throughout the ADV may help shed light on the origin and evolution of similar-appearing landforms on Mars and may also help discern the magnitude and direction of recent climate change on Mars.

Division of ADV microclimate zones: We distinguish three microclimate zones in the ADV on the basis of varying temperature and soil-moisture content: a seasonally dynamic thawed coastal zone, a transitional inland mixed zone, and a stable upland frozen zone.

Zone 1: Coastal thaw zone (subxerous): Soils in the coastal thaw zone exhibit saturated active layers. Relative humidity during summer months averages about 75% [2-4]. Snowfall likely exceeds 80 mm of water equivalent per year. Mean annual air temperature averages about -17ºC [3]. Equilibrium landforms of the coastal thaw zone include, solifluction lobes and terraces and ice-wedge polygons (Fig. 1). Soils are subxerous and contain salts enriched in sodium chloride [4].

Zone 2: Inland mixed zone (xerous): The transitional inland mixed zone includes moderate-to-low-elevation areas in the central Dry Valleys region and high-elevation areas near the coast. Alternating westward-flowing katabatic winds and eastward-flowing winds from the coast produce variable humidity, from 10% to 70%. Mean annual air temperatures are –21 to -25ºC. Meltwater is rare, although some liquid water occurs down from snow banks and glaciers situated on favorable slopes. Snowfall is less than that of the coastal thaw zone [1, 3]. Apart from regions alongside ephemeral streams and isolated snow patches, near-surface soils contain less than 10% soil moisture. The dry climatic conditions of this zone favor the development and preservation of extensive desert pavements, gelifluction lobes, and sand-wedge polygons (Fig. 1). Sand-wedge polygons are similar to the ice-wedge polygons of the coastal thaw zone except that polygon troughs are filled with stratified sand-and-gravel rather than with ice [5, 6] (Fig. 1).

Zone 3: Stable upland frozen zone (ultraxerous): The relative humidity in the stable upland frozen zone averages less than 45% and reflects the predominance of dry katabatic winds [3, 4]. Mean annual temperatures are below -25ºC. Precipitation is rare, but snow blown off the polar plateau accumulates on small glaciers and feeds perennial snow banks in the lee of topographic obstacles. The distribution of snow and ice in the stable upland frozen zone is thus largely related to topography. Meltwater is essentially absent from this microclimate zone and near-surface soils contain < 3% soil moisture. Glaciers and snow banks lose mass by sublimation [7]. The hyper-arid and very cold conditions of the stable upland frozen zone favor the long-term preservation of buried glacier ice. Segregation or vein ice is not an important source of underground ice in this region due to the year-round absence of liquid water. Equilibrium landforms and features in this zone include dry sublimation till (atop debris-covered glaciers) and high-centered, sublimation polygons [8] (Fig.1).

Spatial distribution of microclimate zones and the role of geomorphic overprinting: Landforms originating from thermal contraction in near-surface soils show marked variation among climate zones: ice-wedge polygons occur in the coastal thaw zone; sand-wedge polygons are common in the inland-mixed and stable upland frozen zones; and sublimation polygons are found only in areas where sublimation till rests on near-surface ice in the stable upland frozen zone (Fig. 1). This three-fold geographic distribution of polygon types has remained remarkably stable over the last several million years [1]. For example, there is no evidence for ice-wedge casts in surficial sediments of the stable upland frozen zone. In addition, there is little evidence for extensive debris flows, gullying, or the development of widespread fans (features common in the coastal thaw zone) in the upland frozen zone. Rather, unconsolidated sediments and sublimation polygons of the stable upland frozen zone contain ancient and *in-situ* ashfall deposits (5 to 10 cm from the ground surface) that are suggestive of a paralyzed landscape [1].

Evidence for subtle changes in microclimates: Because each microclimate zone in the Dry Valleys features a unique assemblage of equilibrium landforms, clues to subtle climate variation comes from geomorphic overprinting on base landforms. Examples of such overprinting could be the emplacement of a short-lived active layer (solifluction, gelifluction, and meltwater channel) on partially degraded landforms of the inland mixed or stable frozen upland zones. Similarly, ongoing fluvial dissection of gelifluction lobes in the inland-mixed zone (Fig. 2) is suggestive of current climate warming, bringing geomorphic processes common in the coastal thaw zone inland to the mixed zone. In general, however, the preservation of Pliocene-age sublimation polygons in the stable upland frozen zone of the ADV (without evidence for widespread emplacement of dynamic active layers) indicates long-term climate stability [1].

Applications to Mars: The recognition and documentation of three micro-climate zones within the ADV, the variation of temperature, humidity and soil water content among these microclimate zones, and the identification of equilibrium landforms within these zones, provides important insight into geomorphic processes operating within each ADV microclimate zone. In our opinion, similar climate zones exist on Mars and are largely distributed as a function of latitude-dependent insolation and soil-water content. The detailed knowledge of the processes derived from the ADV microclimates can clearly be

applied to Mars and will be helpful in deconvolving the signal of climatic zonation and climate change there.

There is indeed evidence that Mars has undergone major changes in climate in the recent geological past [9]. These are linked to variations in orbital parameters [10] that result in important variations in ice deposition and stability, and in the emplacement and degradation of 'ice age' deposits extending down to 30° latitude. As another example of recent climate changed deduced from surface landforms on Mars, we are analyzing geomorphologic features displayed on crater interior walls in mid-latitudes (Fig. 3). In Fig. 3, the crater floor displays a rough-textured hummocky surface suggestive of sublimation polygons and eolian modification. At the base of the crater wall, a series of concentric crenulate ridges mark the transition to the crater wall, with the edge of the floor marked by a wall-facing scarp. The ridges become increasingly sinuous toward the crater wall. The main features of the crater wall are alcoves in which blocks and bedrock are exposed, and below this, shallow linear lobate depressions extending to the crater floor. Triangular talus cones form apices at the base of the alcoves, and broaden downslope, filling the shallow linear lobate depressions. We interpret these geomorphologic features as evidence for changing climate on Mars. In this scenario, in the relatively recent geologic past, the climate was sufficiently different to cause the accumulation of snow and ice in the alcoves, leading to the formation of debris covered glaciers that descended toward the crater floor.

Equally informative, and perhaps more analogous to the situation in the ADV, is the variation in "latitude-dependent" landforms on Mars, particularly those related to the dissection of near-surface icy deposits related to the last martian ice age [9]. In this regard, we note that dissection of ice-rich, near-surface debris poleward of 60° N produces features analogous to sublimation tills and sublimation polygons of the upland-frozen zone in the ADV. Equatorward of 60°, dissection of these same icy deposits takes on different characteristics, often resembling landforms common in the intermediate zone of the ADV such as lobate gelifluction lobes. At the current time, equilibium landforms of the coastal thaw zone in the ADV are not well represented on Mars, but the discovery of prominent geologically young gullies in particular latitude bands [11] suggests that similar seasonal melting has occurred in the recent past.

In summary, in a manner analogous to evidence for climate changes discussed previously for the ADV, changing and superposed equilibrium landforms can be used to infer the sign of climate change on Mars. Mapping of similar microclimate zones and their superposition over the critical latitude-dependent transition zones on Mars hold promise for deconvolving the details of geologically recent climate change there (e.g., [9]).

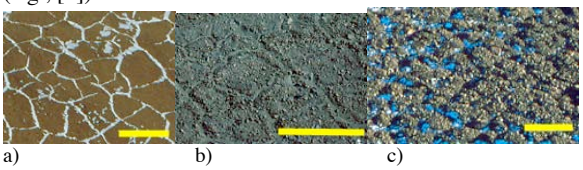

a) b) c)

Figure 1. a) ice-wedge polygons of the coastal thaw zone; b) sand-wedge polygons of the inland mixed zone; c) sublimation polygons of the stable upland frozen zone. Yellow bar is 20 m across in all figures.

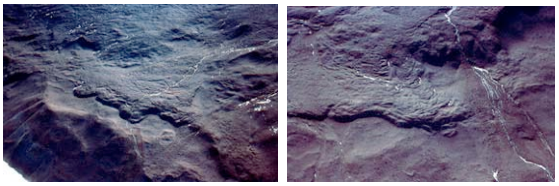

Figure 2. Gelifluction lobes in the inland mixed zone. View is 1 km across (top) and 0.8 km (bottom). Note dissection of lobes by streams. The lobes are > 500,000 yrs old and are now being eroded and incised at unprecedented rates.

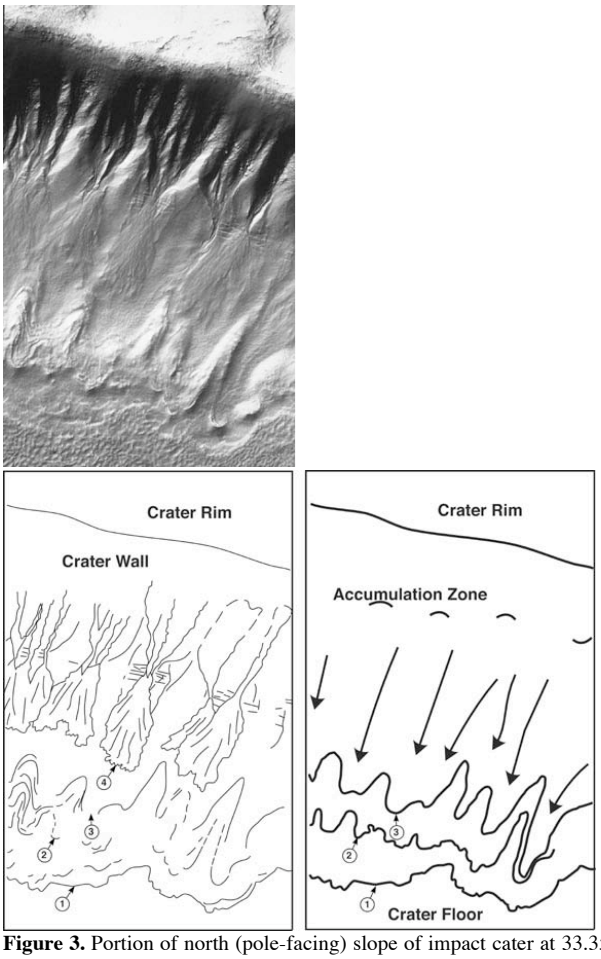

Figure 3. Portion of north (pole-facing) slope of impact cater at 33.35, 195.3W. Top, MOC Image E14 101929. Image is ~3 km width. Bottom left, sketch map of features in MOC image. Bottom right, interpreted directions and sequence of glacial advances represented by the deposits and structures.

References: [1] D.R. Marchant and G.H. Denton, *Marine Micropaleontology*, 27, 253-271, 1996. [2] I.B. Campbell and G.G.C. Claridge, *Geoderma,* 28, 221-238, 1982. [3] W. Schwertdfeger, *Develp. in Atmos. Sci*., 15, 1984. [4] I.B. Campbell and G.G.C. Claridge, *Antarctica: soils, weathering processes, and environment* (Devel. Soil Sci. 16) 368 pp., 1987. [5] T.E. Berg and R.F. Black, *Ant. Res. Ser*. 8, 61-108, 1966. [6] R.F. Black, *Quat. Res*. 6, 3-26, 1976. [7] T.J. Chinn, Proc. Riederlap Workshop; IAHS-AISH Publ. 126, 237-247, 1980. [8] D.R. Marchant et al., *Geol Soc. Am. Bull*., 114, 718-730, 2002. [9] J. W. Head et al., *Nature,* 426. 797-802, 2003. [10] J. Laskar et al., Icarus, 170, 343-364, 2004. [11] M. Malin and K. Edgett, *Science,* 288, 2330, 2000.

EVIDENCE FOR REMNANTS OF LATE HESPERIAN ICE-RICH DEPOSITS IN THE MANGALA VALLES OUTFLOW CHANNEL. Joseph S. Levy[1], James W. Head[1], David R. Marchant[2], and Mikhail Kreslavsky[1]; [1] Dept. Geological Sciences, Brown University, Providence RI, 02912, [2] Department of Earth Sciences, Boston University, Boston, MA 02215.

Introduction: New high-resolution images from MGS and Odyssey reveal an unusual unit on the floor of the Mangala Valles outflow channel. In contrast to abundant terrain showing scour and hydrodynamic shaping typical of the floors and margins of Mangala Valles and other outflow channels [1], this unit is smooth-surfaced, has arcuate and cuspate margins, and has a host of unusual surface features including round pits. We assess several possible origins for this unit and the associated features, and conclude that the most plausible explanation is an ice-rich remnant created by a combination of ponding and ice-cover deflation during the waning stages of the outflow channel flood emplacement.

Description of the Smooth Unit: The smooth unit stretches from the head of Mangala Valles (-18.1 N, 210.6 E) to points at least 400 km north (-11.7 N, 208.8 E), varying in width from up to 10 km to less than 400 m. MOLA altimetry demonstrates that the unit is found predominantly in the deepest regions of the channel; however, in several locations the unit drapes the lower walls of the channel. The margins of the unit are undulatory and rounded in some locations, and scalloped in others, forming arcuate serrations. Where the unit abuts the adjacent walls of the channel, or where there is a contact between the smooth unit and the scoured unit upon which it is superimposed, the relatively level and uniform surface of the smooth unit is beveled. Shadow measurements and MOLA data indicate a minimum thickness of 10-15 m. At the proximal end of the channel, the unit is composed of two layered sub-units, displaying similar morphology but different spatial extents. In several locations the width of the unit decreases towards the distal end of the channel, developing into a tightly braided system several hundred meters wide.

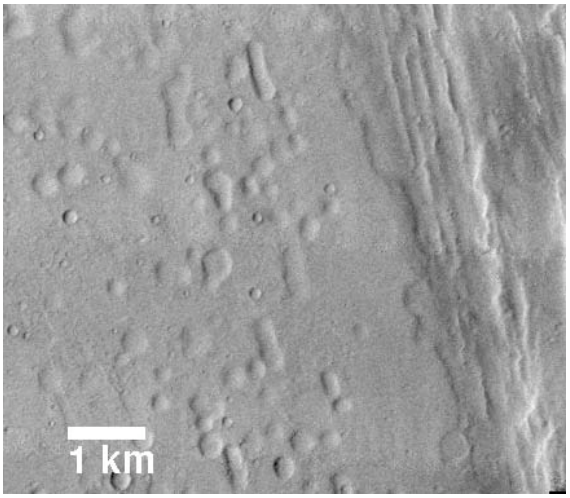

Figure 1. Smooth unit [left] encountering adjacent scoured wall unit [right]. Single and coalesced pits are both visible. From THEMIS image V01454001.

Description of Surface Features: Both the smooth unit and the surrounding scoured terrain are impact-cratered. Primary impact craters are distinguished by raised rims and generally circular shape. Craters range in diameter from 20-560 m. Impact crater counts between the two surfaces are generally similar, with the scoured terrain appearing slightly older than the superimposed smooth unit.

The most striking features observed on the smooth unit are abundant, shallow, round pits. We measured the diameters of all 404 pits and 2137 craters in THEMIS images V01454004, V0440003, and V04762003. The pits range in diameter from 100-600 m, with a mean of 230 m and standard deviation of 60 m. Large, angular boulders are found at the center of many pits near the proximal end of the channel. Most of the pits with blocks have a marginal raised rim, however, none of the empty pits have raised rims. Pits with blocks tend to be larger than empty pits; however the largest pits are empty [Figure 1 and 3].

The pits are predominantly circular; however, clusters of pits show signs of coalescence, forming elongated rectangular depressions with rounded short sides and long axes sub-parallel with the channel. There is no spatial preference for pitting density.

Several channels < 100 m in width are associated with the smooth deposit at its margin. These meandering channels are all less than 6 km in length [Figure 2]. Similarly, two features resembling small channels trace circuitous paths at the head of the channel [Figure 3].

Discussion and Interpretation: On the basis of these observations, we interpret the smooth unit as an ice-rich residue created by a combination of ponding of flood water and ice-cover deflation during the waning stages of the outflow channel flood event. The presence of the unit in the deepest reaches of the channel supports a ponding hypothesis [2], while the draping of the unit over scoured terrain suggests deflation of an ice cover, as would have formed atop an outflow flood under cold, dry conditions [3]. We interpret the observations to mean that in the early

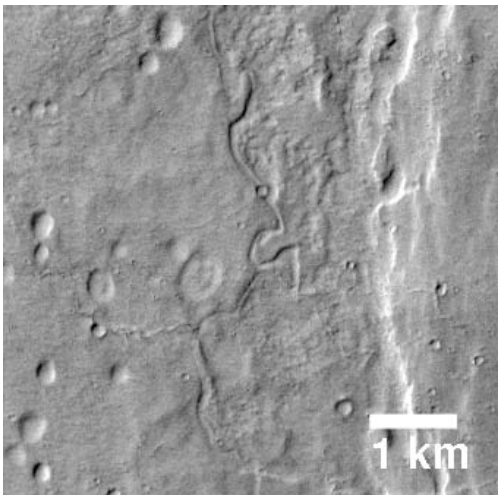

Figure 2. Channel at the margin of the smooth unit [left]. From THEMIS V044000003.

stage, the ponded material and ice-cover froze solid and sublimated, leaving the deposit as a sublimation residue. Locations showing two sub-units of smooth terrain may be areas where an ice-rich cap settled over a debris rich pond, leading to a more heavily degraded ice-rich upper unit, and a less degraded debris-rich lower unit [4]. The lack of elongated craters or streamlines argues against a flowing-ice or glacial ice origin for the unit.

The size-frequency distribution of the pits rules out the possibility that the pits are caused primarily by degradation of impact craters on an ice-rich surface. Rather, the pits in the smooth unit are interpreted as thermokarst-like features, similar to *alases*: terrestrial thermokarst pits [5]. Whereas terrestrial *alases* form through a combination of melt, flow, and evaporative processes, resulting in the lowering of ice-rich terrain, the martian features are interpreted as sublimation pits. Both terrestrial *alases* and martian sublimation pits form when the thermal equilibrium of an ice-rich unit is disrupted, leading to enhanced, localized melting or sublimation [4]. Pits may also be kettles left over from ice-blocks carried downstream by outbreak flood flow [9].

The scalloped or serrated texture of the smooth unit margin is explained as localities where sublimation pits formed near the margin of the unit. Longer embayments may be locations where several sublimation pits coalesced, forming an elongated cavity. Sublimation could be enhanced by scarp formation and marginal wasting.

In areas where the unit thins and adopts a meandering aspect, some sort of esker-like genesis is implied by the braided morphology. Esker-like deposits imply significantly greater ice-cover of the surface than is presently observed, as well as the sub-ice flow of sediment-laden liquid water. These conditions are not inconsistent with those associated with the freezing of debris-rich, ponded flood water.

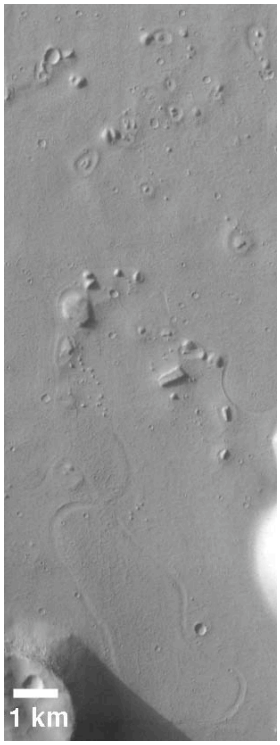

Figure 3. Pits with large blocks, and channel-like features at the head of Mangala Valles. From THEMIS V04762003.

The presence of pitting even within the thin portions of the deposit suggests that the esker-like formations also contain extant ice, however, the diminutive nature of the deposit suggests that it may be even more debris-rich than the bulk of the smooth unit.

Conclusions: The identification of an ice-rich residue associated with an outflow flood event strongly suggests that this outflow event occurred on a cold and dry Mars, consistent with other observations of the same area of Mangala [10]. Further, the preservation of ice-rich debris beneath a sublimation till suggests that climate conditions have remained cold and dry on Mars for at least the past several billion years, and that flood residue can be maintained for unprecedented periods of time. The formation of extensive sublimation pits strongly suggests that parts of the remaining deposit are currently ice-rich, making this deposit a primary target in exobiological and ancient climate investigations.

References: [1] Malin & Edgett (2001) *JGR*, 106 23,429-23,570. [2] Lucchitta & Ferguson (1983) *JGR*, Supp. 88 A553-A568. [3] Wallace & Sagan (1977) *NASA Tech. Mem.* X-3511, 161. [4] Washburn (1973) Periglacial Proc and Env. [5] Soloview (1973) *Biuletyn Peryglacjalny*, 23, 135-155. (6) Turtle et. al, [2001] *LPSC32* #2044. [7] Hartmann (1977) *Icarus*, 31;2, 260-276. [8] Hartmann & Neukum (2002) *Space Sci. Rev.* 96: 165-194. (9) Benn & Evans (1998) *Glaciers and Glaciation,* 618. [10] Head et al (2004) *GRL*, 31, 40701.

REGIONAL MID-LATITUDE LATE AMAZONIAN VALLEY GLACIERS ON MARS: ORIGIN OF LINEATED VALLEY FILL AND IMPLICATIONS FOR RECENT CLIMATE CHANGE. James W. Head[1], David R. Marchant[2], Marshall C. Agnew[1], Caleb I. Fassett[1], and Mikhail A. Kreslavsky[1]. [1] Dept. of Geological Sciences, Brown University, Box 1846, Providence, RI 02912 USA (James_Head@brown.edu); [2]Dept. of Earth Sciences, Boston University, Boston, MA USA.

Introduction. Among the hallmark morphologies of the highland-lowland boundary region in the northern mid-latitude Deuteronilus-Protonilus Mensae area (30-50°N, 315-350°W) is the fretted terrain (1), consisting of 1) debris aprons that surround many of the massifs and valley walls, and 2) lineated valley fill (LVF) that occurs on the floors of many of the valleys (2-14). The ages of these deposits are typically much younger than the adjacent plateau terrain or its breakup and the formation of the valleys themselves (e.g., 9, 14). The margins of the debris aprons consist of rounded and convex upward topography, and at Viking resolution the debris aprons and the valley fill can appear smooth and relatively homogeneous or, in contrast, can be characterized by closely spaced parallel ridges and grooves a few to several tens of meters high. These sets of parallel ridges have been interpreted to have formed both parallel and normal to valley and mesa walls. Some workers (e.g., 2) argue that the lineations form mostly normal to flow due to converging flow from debris aprons on opposite sides of valleys or mesas, while others (e.g., 4) argue that bending of ridges and grooves entering valleys from a side tributary supports flow in the direction parallel to the valley. Recent analysis shows variable downslope gradients suggesting that lateral flow was minimal (e.g., 11). All agree that the materials represent some sort of viscous flow processes, but opinions differ on the details of the mechanism; most authors call on processes of gravity-driven debris flow, assisted by ice or water in the interstices derived from either groundwater or diffusive exchange with the atmosphere (e.g., see 7, 10, 13-14). Some liken the process to rock-glacial flow (e.g., 2, 4) with the source of the lubricating agent being ice from atmospheric frost deposition and diffusion (2) or mobilized interstitial ground ice (4).

New Observations. New THEMIS, MOLA and MOC data provide additional perspectives on the origin of the lineated valley fill, suggesting that at least in some areas, glaciation (accumulation of snow and ice to sufficient thickness to cause its local and regional flow) has played a significant role. We have analyzed numerous areas along the dichotomy boundary north of 30 degrees north latitude and present the results from one area as an example. In this region (Fig. 1) in southern Deuteronilus Mensae, a T-shaped valley occurs just south of a large depression. The walls of the large depression are characterized by debris aprons and there is a break in the southern rim of the depression that leads to the top of the T-shaped valley (about 100 km across). A topographic profile (Fig. 2) from the floor of the large depression across the southern wall, across the top of the T and along the vertical part of the T shows 1) the flat floor of the large depression, 2) the classic convex upward slope of the debris apron, 3) the elevated floor of the top of the T, 4) the convex upward slope of the vertical part of the T. Note that the floor of the T-shaped valley along the top of the T lies at elevations as high as -2600 m, almost a kilometer above the large depression floor. The bottom of the valley along the vertical part of the T lies ~500 m below the valley floor at the top of the T.

THEMIS data superposed on MOLA altimetry and viewed perspectively show strong evidence for flow lineations (Fig. 3), their characteristics and their directions; details of the lineations are shown in the MOC images (Figs. 4-6). Examination of Figs. 1 and 3 shows a 20 km diameter breached crater south of the eastern arm of the T. Numerous lineations on the floor of the crater converge and can be traced through the gap in the crater wall (Fig. 4, upper right) joining lineations beginning at the eastern edge of the T (Fig. 4, lower left). Similar lineated valley fill extends from the mouth of a north-trending valley in the lower western part of the T, is deformed by valley lineations from valley fill apparently moving from the higher terrain to the west, and then joins the general lineated valley fill just to the east (Fig. 5). Furthermore, additional lineated valley fill begins at the base of the broad ampitheater on the western part of the top of the T, and converges with at the T-junction with the lineated valley fill coming from the west and the east (Fig. 3). From here, these three major flow lineation directions converge and extend down the vertical part of the T, with many of the lineations contorted at the margins of the convergence (Fig. 6). At the end of the major lobe, the topography is broadly convex upward (Figs. 2, 3) and the perspective view (Fig. 3) shows the distinctive lobe-like nature of the valley fill as it extends into the adjacent low-lying terrain.

Origin of Lineated Valley Fill. What processes are responsible for the valley fill? These lineations and their complex patterns resemble flow lines in glacial ice on Earth, particularly where glacial ice converges from different directions at different velocities and deforms into complex patterns (compare Figs. 3-6, Mars, and 7, Earth). Detailed analysis of the MOC, THEMIS and MOLA data suggests that changing environments and local topographic conditions (such as the crater walls and the narrow valleys) favored accumulation and preservation of snow and ice, and its glacial-like flow down into surrounding areas for distances approaching 70 km. Such environments are typical of snow and ice accumulation and debris-covered glacial flow in the Antarctic Dry Valleys, a cold polar desert analogous to the environment on Mars and in regional valley glaciers in Baffin Island (15). Alternative hypotheses for the lubrication and flow of rock debris focus predominantly on groundwater, ground ice or ice from atmospheric water vapor diffusion (e.g., 2, 4, 7, 10, 13-14). We believe that the thickness of the deposit, the great lateral extent and continuity of flow lineations, and their complex interactions consistent with glacial-like flow, are all evidence that supports glacial-like flow of debris-containing ice, rather than ice-containing debris. The relationship between the lineated valley fill and the debris aprons is not yet firmly established; however, the contiguous nature of many examples of lineated valley fill and debris aprons (Fig. 1) suggests that if the glacial interpretation of the valley fill is supported by further observations, then glacial ice may play more of a role in the formation of debris aprons than previously suspected (see also 16-17). The age of the deposits in this region are Late Amazonian (~300 Ma, with some of the deposits as young as 10 Ma (14)), broadly similar in age to the tropical mountain glaciers of Tharsis Montes and Olympus Mons (16-19). This suggests that there may have been periods during the Amazonian when tropical and mid-latitude glaciation was extensive. Significant amounts of ice could remain today in these valleys beneath a protective cover of sublimation till (e.g., 20).

Conclusions. Breached upland craters and theater-headed valleys reveal features typical of terrestrial glacial accumulation zones, parallel lineations on valley floors resemble flow lines in glacial ice, converging lineations resemble ice flow through constrictions, and complex

chevron-like flow patterns occur where lineated valley fill converges from different directions. This example in the Deuteronilus Mensae region shows an integrated pattern interpreted to represent snow and ice accumulation and flow for ~70 km and resembles valley glacial systems on Earth in major morphology, topographic shape, planform and detailed surface features. These data imply that during the Late Amazonian, significant climate change occurred to cause sustained snow and ice accumulation and flow at mid-latitudes to form a regional system of valley glaciers [22].

References. 1. R. Sharp (1973) *JGR*, 78, 4073; 2. S. Squyres (1978) *Icarus*, 34, 600; 3. S. Squyres (1979) *JGR*, 84, 8087; 4. B. Lucchitta (1984) *JGR*, 89, B409; 5. R. Kochel & R. Peake (1984) *JGR*, 89, C336; 6. M. Carr (1995) *JGR*, 100, 7479; 7. M. Carr (1996) *Water on Mars*, Oxford, 229 p.; 8. A. Colaprete & B.Jakosky (1998) *JGR*, 103, 5897; 9. G. McGill (2000) *JGR*, 105, 6945; 10. N. Mangold & P. Allemand (2001) *GRL*, 28, 407; 11. M. Carr (2001) *JGR*, 106, 23,571; 12. M. Malin & K. Edgett (2001) *JGR*,106, 23439; 13. N. Mangold et al. (2002) *PSS*, 50, 385; 14. N. Mangold (2003) *JGR*, 108, 10.1029/2002JE001885; 15. D. Benn & D. Evans (1998) *Glaciers and Glaciation*, Arnold, 734 p.; 16. G. Neukum et al. (2004) *Nature*, 432, 971;17. J. Head et al. (in press) *Nature*; 18. S. Milkovich & J. Head (2003) *6th Int. Mars Conf.* abstr. 3149; 19. J. Head & D. Marchant, (2003) *Geology*, 31, 641; 20. J. Head et al. (2003) *Nature*, 426, 797; 21. A. Post & E. Lachapelle (2000) *Glacier Ice*; 22. J.Head et al. (2005) *LPSC*. this volume.

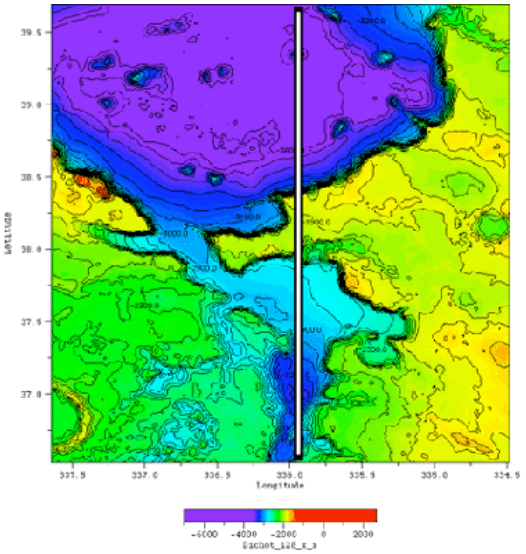

Fig. 1: Color-coded MOLA Altimetry; line shows location of profile.

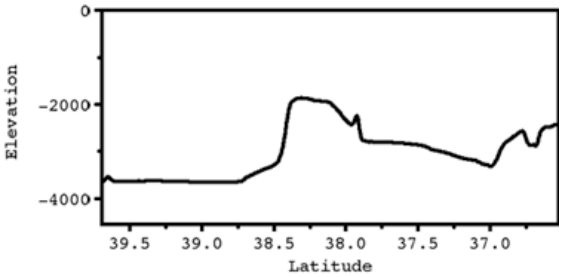

Fig. 2: Altimetric profile (location, Fig. 1).

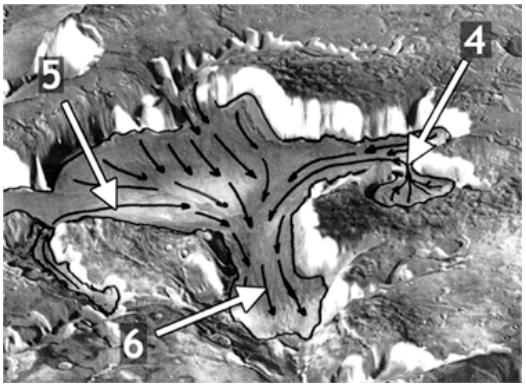

Fig. 3: THEMIS IR on MOLA Altimetry; perspective view from south.

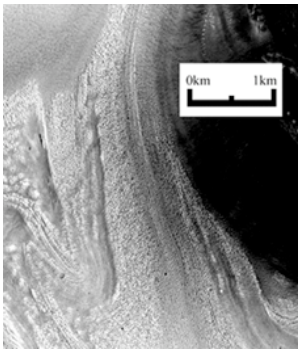

Fig. 4: MOC image of LVF detail (location, in Fig. 3).

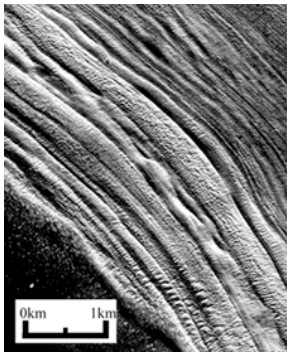

Fig. 5: MOC image of LVF detail (location, Fig. 3).

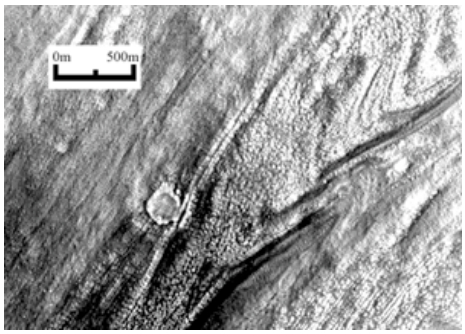

Fig. 6: MOC image of LVF detail (location, Fig. 3).

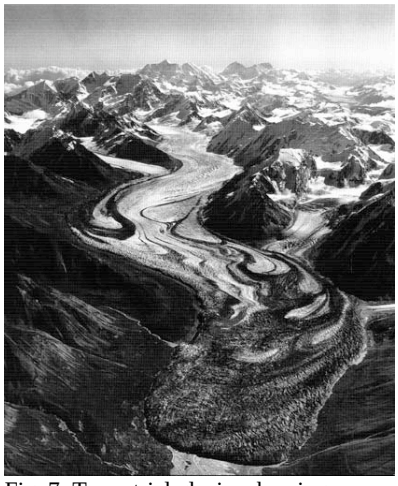

Fig. 7: Terrestrial glacier showing features analogous to those observed in Figs. 3-6 on Mars (21).

BEYOND THE EQUILIBRIUM PARADIGM – GLACIAL DEPOSITS IN THE EQUATORIAL REGION OF MARS. J. Helbert[1] and J. Benkhoff[1,2], [1]Institute for Planetary Research, German Aerospace Center DLR, (Rutherfordstr. 2, Berlin-Adlershof, Germany, joern.helbert@dlr.de), [2]Research and Scientific Support Department, ESTEC, (Keplerlaan1, 2201AZ Noordwijk ZH, The Netherlands).

Introduction: While Mars has been considered for a long time a dry place except for the early Noachian, this view has changed in recent years. This started mainly after the MOC imagery showed features like the gullies and morphological features which can be associated with glacial activity. Now the motion was discussed that at least small amounts of water or ice had been present in the recent past on Mars. Still, the common notion was that Mars today is a dry place. With the excellent dataset of the Gamma and Neutron spectrometer (GRS and HEND) on board of Mars Odyssey this view had to be corrected. The instrument detected water abundance of at least 8wt% in the equatorial regions of Mars and this water is found within the first 2m below the surface, the penetration depth of the instrument.

Recent results by MarsExpress: Since January 2004 the High Resolution Stereo Camera (HRSC) on MarsExpress reports mounting evidence for very recent glacial activity in the equatorial regions of Mars. At the same time the Planetary Fourier Spectrometer reports localized enhancements in the near surface atmospheric water abundance. We will dicusss scenarios which can explain these observations based on the assumption of longtime stable equatorial ice deposits.

Water on Mars: There are three main explanations for the observed amount of water which are not mutually exclusive. Some of the water measured is most likely adsorbed water. While it is still unclear how much water the Martian soil can adsorb, this mechanism can not explain the high abundances measured in some place. We might see highly hydrated minerals. Some of the suggested minerals are indeed capable of holding large quantities of water. The last and maybe most exciting possibility are near surface ice deposits. However if it is ice, the question is, how did it survive close to the surface under the hyper-arid conditions we encounter on present day Mars. And how much ice is there really on present day Mars?

Ice on Mars: Until today we have seen ice only at the polar caps and only this year did we get the first direct measurements of ice abundances by the PFS and OMEGA instrument on Mars Express. We do not have any direct evidence for ice at lower latitudes. From the GRS and HEND measurements we know that the polar caps extend under the surface much further than previously expected. One might assume therefore that near surface ice deposits we see at low latitudes are literally only the tip of an iceberg and the Mars might have a global ice reservoir in shallow depths. If this would be the case, Mars would be a wet planet which is just temporarily frozen. Another less dramatic scenario is the assumption that ice deposits at low latitudes are remnants of the last Martian ice age. The change in the obliquity of Mars can lead to a redistribution of ice across the planet. So maybe we observe today a transition state, in which we only see the dwindling remains of equatorial glaciers. If the ice within the top 2m has survived until today, this would however imply that these regions have been covered by large amounts of ice during the last ice age. Both ice related scenarios would imply that Mars has, or at least had in the very recent past, large quantities of ice on or close to the surface. It implies further that Mars is not in a steady stat, but has a active climate with global variations on several different time scales.

The Berlin Mars near Surface Thermal model: Over the recent years we have developed the Berlin Mars near Surface Thermal model (BMST) to address this question [1]. Most models used up to now assume a thermophysical steady state for the Martian soil. Under such conditions ice could not be stable close to the surface in equatorial regions. However modelling shows that the obliquity of Mars changes dramatically over time [2]. There are observational evidences showing at least two climatic cycles on Mars. There is a long term cycle in the order of 5-10 Mio. years as shown evidence of glaciation in equatorial regions [3] and a medium term cycle in the order of 100-300ka as shown for example by the layering in the polar caps [4].

The BMST is focused on studying the stability of recently deposited ice. Our model is based on a layered structure of the subsurface material, in which each layer can have different physical and thermo-physical properties. The main features of the BMST are a high lateral resolution down to the centimeter range, the realistic treatment of the thermal properties of ice-rock mixtures, a detailed treatment of gas flux within the surface and into the atmosphere and a variable temporal resolution which allows to study daily as well as annual variations. Using the model we can study the redistribution of volatiles with the subsurface over time. This allows to predict limits for the burial depth of ice assuming non-equilibrium conditions.

Terra Arabia: The SWC channel of the PFS instrument on MarsExpress has detected an enhancement in the atmospheric water vapour content close to the

surface over Terra Arabia [5]. Interestingly this is one of the equatorial areas in which GRS on Mars Odyssey reports an increased water content in the soil [6]. The HEND instrument of the GRS instrument suite reports a water abundance of 12 wt% below an at least 19cm thick layer of dry soil [7]. We will show a scenario in which ice placed in Terra Arabia during a recent ice age in Mars is indeed stable within 1m below the surface over several 10ka. GCM calculations as done for example by [8] show, that during phases of higher obliquity larger amounts of high can be deposited in this area. The ice deposit is protected until present time by a lag deposit consisting of a layer of very fine, bright dust with a very low thermal conductivity. We find this dust layer in one of the area which geographical coincides with the areas showing the highest content of water in the soil in GRS measurements. While such a long time stable ice deposit would explain the GRS observations, it contradicts the observations by PFS. However we have identified adjacent areas in which ice might have migrated downward after deposition on or close to the surface. This downward migration can lead to the formation of an ice lens within the first few meters below the surface. The modelling shows that a destruction of this ice lens by sublimation can lead to a significant increase of water vapour being released in the atmosphere. This might by observed by PFS right now.

Hecates Tholus: An analysis of data obtained by the HRSC camera on MarsExpress revealed morphological evidence for the existence of glacial deposits on the flank of Hecates Tholus [3]. Their ages derived from crater counts are about 5 to 24 million years. We have studied the stability of glacial remenants from the last Martian ice age in this area.

Summary: We will show, that even in the equatorial regions of Mars ground ice deposits can be stable over long periods of time. The main assumption we have to do is, that the near surface layer of Mars is not in an equilibrium state.

There are mounting evidences of Martian climate cycles on different time scales. One of the shortest time scales indicated by the layering in the polar caps is in the order of only several 10ka.

References: [1] Helbert and Benkhoff, JGR, 2003 [2] Laskar et al., Icarus, 2004. [3] Hauber et al., Nature 2004. [4] Milkovich et al. 2004 [5] Formisano et al. 2004 [6] Boynton et al. 2003 [7] Mitrofanov et al. 2003 [8] Haberle et al. 2004

Additional Information: This work was supported by the German Research Council (DFG) under grant BE 1630/2.

MARS ODYSSEY NEUTRON SPECTROMETER WATER-EQUIVALENT HYDROGEN: COMPARISON WITH GLACIAL LANDFORMS ON THARSIS. R. C. Elphic[1], W. C. Feldman[1], T. H. Prettyman[1], R. L. Tokar[1], D. J. Lawrence[1], J. W. Head, III[2], S. Maurice[3], [1]Space Science and Applications, Los Alamos National Laboratory, Los Alamos, NM 87545 (relphic@lanl.gov), [2] Department of Geological Sciences, Brown University, Providence, RI 02912, [3] Centre d'Etude Spatiale des Rayonnements (CESR), 31400 Toulouse, France.

Introduction: We have previously described an enhancement of water-equivalent hydrogen (WEH) derived from Mars Odyssey neutron spectrometer (NS) observations on the western slopes of Olympus Mons and the principal Tharsis Montes [1]. Recent results from the High Resolution Stereo Camera aboard Mars Express have reinforced the idea that relict water ice may still underlie certain landforms on the western slopes of Olympus Mons [2,3], and possibly the other volcanoes as well. There is abundant evidence of the past possible presence of cold-based mountain glaciers [4,5], resulting from significant snow/ice deposits in these locations during periods of high obliquity [6,7], based on global climate modeling. Here we investigate whether or not the NS data support enhanced WEH associated with previously identified glacial and periglacial landforms.

Neutron Spectrometer Observations: Measurements of the epithermal neutron leakage flux out of the martian surface and atmosphere have been analyzed and a minimum water-equivalent hydrogen (WEH) map (assumed to be homogeneously mixed with dry soil throughout the depth of sensitivity) has been derived [8]. For the Tharsis region, WEH ranges between 2 and 8 wt%. The western slopes of Olympus Mons, and the Tharsis Montes have higher WEH abundance than the eastern slopes. There are also enhanced WEH abundances centered on Noctis Labyrinthus and western Valles Marineris. Even higher WEH abundances are found further to the west, trending into Amazonis Planitia and the Medusae Fossae Formation, also potential sites of volatile-rich deposits on the basis of geological analyses [9,10].

NS Data Deconvolution: The NS footprint has a FWHM of ~600 km, or about 10° of arc on the surface. This response function smears out features that are smaller than the footprint, including possible water-bearing deposits considered here. Instead, we may see a smeared-out regional high.

The NS footprint for epithermal neutrons is large but well characterized, and the statistics of the data are good. So we can attempt to deconvolve the mapped epithermal fluxes in order to improve the spatial resolution of the inferred WEH. We initially sum a full Mars year of NS data in small spatial bins (15 km). These data have been normalized to cosmic ray and seasonal atmospheric variations [11]. We then smooth the raw, summed count rates with a gaussian filter of approximately 220-km FWHM. The final step is to 'sharpen' the smoothed map using an iterative deconvolution technique similar to Jannson's, $I_{k+1} = I_k + r\,(O - p \otimes I_k)$, where I_{k+1} is the current estimate of the restored image, I_k is the previous estimate, r is a relaxation function, O is the original smoothed image, p is the total effective point spread function (equivalent to the Gaussian smoothed NS response function), and $\otimes$ denotes a convolution operation. The relaxation function r serves to constrain restored image estimates to physically reasonable values, for example non-negative values.

Geology and Relationship to WEH: The Tharsis Montes edifices consist mainly of lava flows and ash deposits (as well as eolian mantle) [12], but there are distinctive units to the west and northwest of the three major volcanoes that have been interpreted to be of glacial origin in part or in whole [4,12,13,14]. Models of snow and ice accumulation on the Tharsis Montes and resulting glacial transport have also been created [15,16]. The three facies of these Tharsis Montes glacial units relevant to our study are: R, the outer ridged facies, which may be ice-cored drop moraines; K, the knobby facies which may be sublimation till covering ice; S, the smooth facies which may be rock glacier deposits. The smooth facies may be the youngest, with the smallest depths-to-ice. The combined outlines of the three facies for each glacial unit are shown on panel D of Figure 1.

Panel A of Figure 1 shows the original smoothed map of epithermal count rates for most of central Tharsis, centered on 0º latitude and 115º W. Panel C shows the derived WEH map corresponding to panel A. Panel B shows the result of our deconvolution scheme, after 20 iterations, and Panel C is the corresponding WEH map. Note the considerable enhancement in WEH estimates in (D) vs. (C). Areas of comparable or higher WEH are found outside the glacial units. Nevertheless, apparent WEH values in excess of 6 wt% H_2O on the western flanks of the Tharsis Montes are consistent with the epithermal neutron flux data.

Discussion: If a simple stratigraphic model of pure ice overlain by relatively desiccated (2 wt% WEH) sublimation till is applied, the depth to ice consistent with these values is less than 60 cm. We are currently developing a forward model of the MO NS response to

shallow buried ice limited to the facies discussed earlier. Clearly this modeling must include the effects of water ice or hydrous minerals in surrounding areas. However, our results suggest that the Neutron Spectrometer is detecting evidence of buried ice in these Late Amazonian aged tropical mountain glaciers. Higher resolution NS data (e.g., an aerial platform) and NS instrumentation on surface rovers provide promising avenues to further investigate these important resources.

References: [1] Elphic, R. C., et al., (2004) *LPS XXXV*, abstract #2011. [2] Basilevsky, A.T. et al. (2005) *LPS XXXVI*, abstract #2005. [3] Neukum, G., et al., (2004) *Nature*, *432*, 971-979. [4] Head J. W. III and Marchant D. R. (2003) *Geology*, *31*, 641-644. [5] Milkovich, S. E. and Head, J. W. (2003) *6th International Conference on Mars*, abstract #3149. [6] Mischna, M. (2003) *JGR-Planets, 108,* 5062, doi:10.1029/2003 JE002051. [7] Haberle, R. M., et al., (2004) *LPS XXXV*, abstract #1711. [8] Feldman, W.C. et al., (2004) *JGR-Planets, 109*, doi:10.1029/2003JE002160 [9] Head, J. W. and Kreslavsky, M. *LPS XXXV*, 1635, 2004. [10] Head, J. W. et al. (2003) *Geophys. Res. Lett., 30* (11), 1577, doi:10.1029/2003GL017135. [11] Prettyman T. H., et al. (2004) *JGR, 109(E5)*, E05001. [12] Scott, D. H. and Tanaka, K. L. (1986) *USGS map I-1802-A.* [13] Lucchitta, B. K. (1981) *Icarus, 45,* 264-303. [14] Scott, D. and Zimbelman, J. (1995) *USGS Map I-2480*. [15] Shean, D. E. et al. (2004) *LPS XXXV*, abstract #1428. [16] J. Fastook, J. Head, D. Marchant and D. Shean (2005) *LPS XXXVI*, abstract #1212.

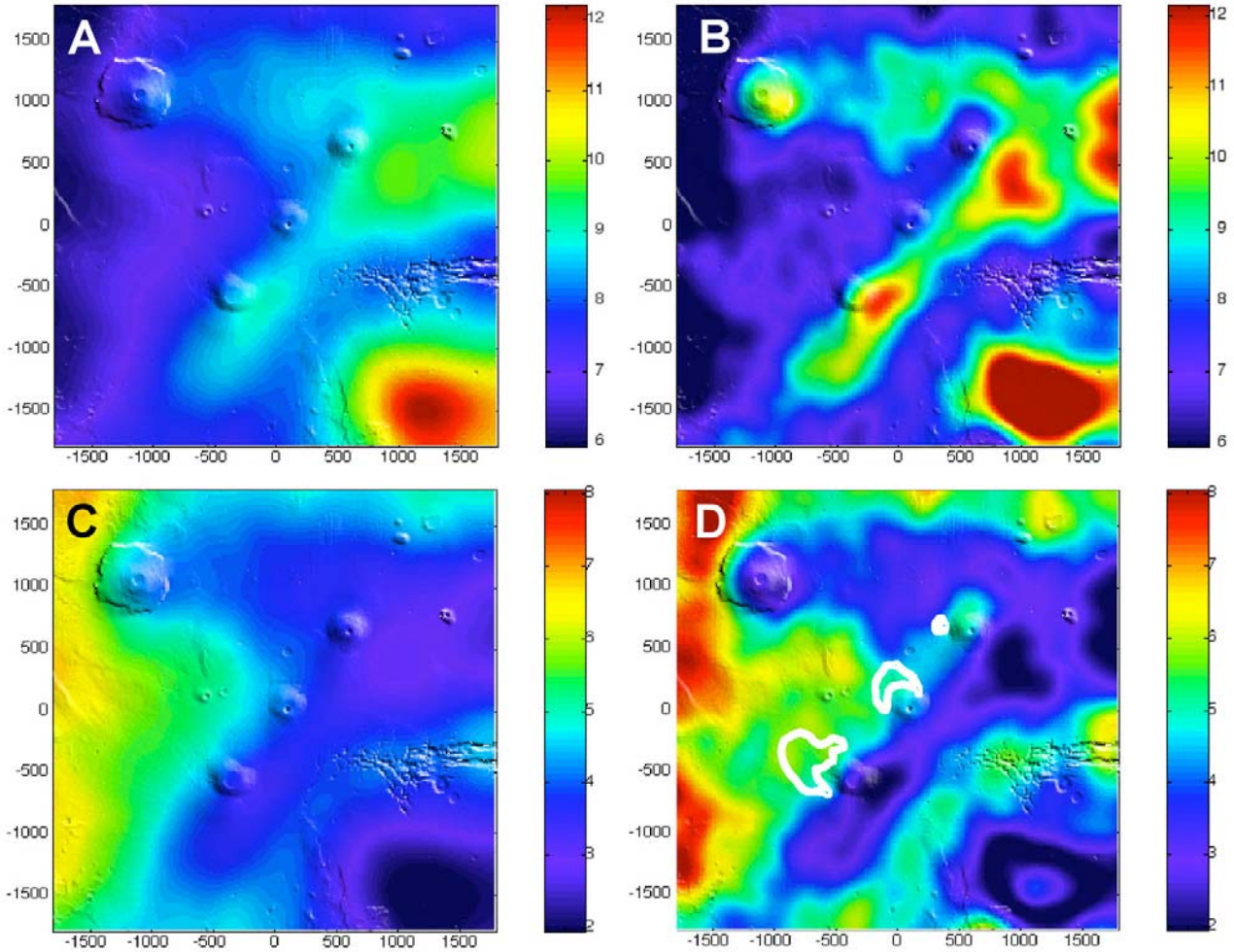

Fig. 1. (A) Original smoothed epithermal neutron count rate map superimposed on MOLA topography, centered on 115 W; (B) Deconvolved epithermal count rate map; (C) Corresponding WEH (wt%) for Panel A; (D) Corresponding WEH for Panel B, with outlines of the combined facies (S, R, K) of the glacial units shown in white.

ICE SHEET MODELING: MASS BALANCE RELATIONSHIPS FOR MAP-PLANE ICE SHEET RECONSTRUCTION: APPLICATION TO THARSIS MONTES GLACIATION. J. L. Fastook[1], J. W. Head[2], D. R. Marchant[3] and D. E. Shean[2], [1]Climate Change Institute and Computer Science, Univ. Maine, Orono ME 04469 (fastook@maine.edu), [2]Dept. Geol. Sci., Brown University, Providence RI 02912, [3]Dept. Earth Sci., Boston University, Boston MA 02215.

Introduction: Deposits on the flanks of the large Tharsis Montes volcanoes (Arsia, Pavonis, and Ascraeus Mons) have been recognized to be of glacial origin [1,2]. These Amazonian-aged deposits display three distinct facies, ridged, knobby, and smooth [3], each of which can be associated with different glacial processes [1]. The outermost ridged facies is thought to be the imprint of ice-margin drop moraines recording the fluctuations of a stable cold-based ice sheet. Inside this is the knobby facies, interpreted as a sublimation till deposited as the ice sheet sublimated during a period of major contraction of the ice sheet. Finally, contained within both of these is the smooth facies which may contain debris-covered glacial ice, similar to rock glaciers found in the Dry Valleys of Antarctica [1]. The deposits form fans trending to the northwest from each of the volcanoes and have been described elsewhere [1-4]. Steady-state flowband profiles have been shown to produce reasonable ice sheet configurations of a few hundred to a few thousand meters thickness. However, flowband modeling [5,6] makes estimates of volumes difficult, and steady-state modeling does not allow for the possibility that these ice sheets never attained full equilibrium configurations during the transient climatic conditions that accompany the large oscillations in obliquity that dominate the Martian climate [7].

Modeling Postulated chronologies for ice sheet behavior are emerging as a better understanding of Mars climate change driven by major variation in the obliquity is seen as allowing for ice sheets to form near the equator at high elevations on the flanks of the large volcanoes [1]. Ice sheet models, coupled with reasonable assumptions about the climate, can obtain estimates for the volumes of these ice sheets, better constraining the water budget for the planet [5,6]. Ice sheet models usually involve an integrated momentum-conservation equation based on the flow law of ice [9] coupled with a mass-conservation, or continuity equations to yield a differential equation for ice extent and thickness as a function of time [10,11].

Mass Balance Distribution Such an equation requires specification of the source of this mass at each point in the domain, the so-called mass balance. The mass balance consists of two parts, the annual accumulation (ice-equivalent snowfall, in m/yr) and the annual ablation (melting, sublimation, or other erosive processes that remove ice from the ice surface). The difference between these two is the net mass balance, which is the source (or sink if negative) in the continuity equation.

On Earth the mass balance can be measured for existing ice sheets, but for reconstruction of paleo-ice sheets a parameterization in terms of elevation and location on the planet is usually used. The accumulation part of the mass balance is usually taken to be proportional to the saturation vapor pressure, a measure of how much water the atmosphere can hold. The saturation vapor pressure is an exponential function of temperature, with a cold atmosphere holding much less water, and hence able to produce much less snow. We would expect the Martian situation to be similar.

On Earth, for most glaciers the ablation component is typically due to surface melting with liquid runoff from the ice sheet. This is calculated by imposing a seasonal amplitude onto the mean annual temperature at a location and counting positive degree days. The melt rate is proportional to the number of positive degree days. Since the Earth is colder at higher elevations (the so-called lapse rate, usually linear) we usually see small positive mass balance at high elevations (cold, little snow, but no melting), large positive mass balance at mid elevations (warmer, so more snow, but still little melting), and then strongly negative mass balance at low elevations (warm, so plenty of snow, but much more melting). This leads to snow-capped mountains and highland growth of glaciers, with the concept of an equilibrium line (mass balance positive above and negative below).

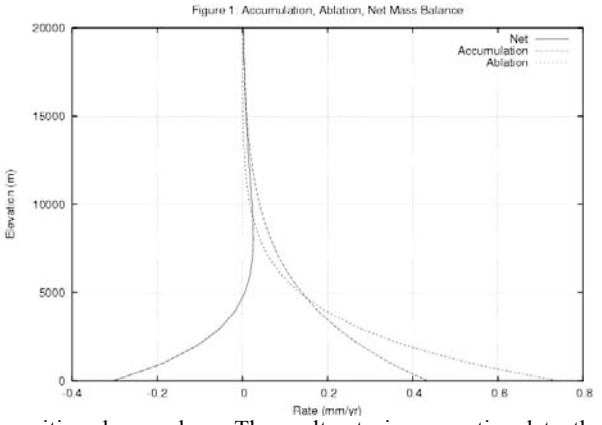

On Mars, the temperature seldom reaches the melting point of water ice, the lapse rate is much smaller, and the dominant mechanism for mass removal is by sublimation. Two sublimation mechanisms are defined [12,13], buoyancy- and turbulence-driven. Both depend on the saturation vapor density (itself the saturation vapor pressure divided by the total pressure) and hence have the same exponential dependence on temperature as the accumulation component of the mass balance. With a lapse rate, falling temperature with elevation leads to declining accumulation and sublimation rates. With pressure in the denominator, sublimation declines less rapidly, leading to overall lower, and possibly negative, net mass balance. Thus on Mars we might expect snow-filled valleys rather than the snow-capped mountains we see on the Earth. Declining relative humidity, increasing ventilation (both of which affect sublimation),or some melting at lower elevations can lead to net negative mass balance at low elevation. Thus we might have two equilibrium lines (Fig. 1), a high and a low one, with positive mass balance only in between.

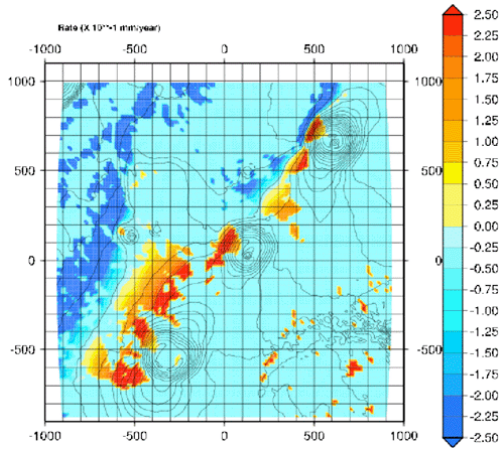

Figure 2. Modeled mass balance.

Spatial Distribution: All of this produces a mass balance distribution that depends on elevation, but the fan-shaped deposits are all on the northwest flanks of the volcanoes. This may be due to a snow tail in the lee of the volcanoes or to a cloud shadow that reduces ablation, or even to orographic effects as air masses move up the volcano slopes [e.g. 15-18]. Whatever the cause the climate parameterization needs some way to produce spatially non-uniform mass balance. One way to do this is to only allow accumulation where the surface slopes in a particular direction. We form the dot product between a unit vector in a specified direction (northwest) with a unit vector in the direction of the surface gradient (the cosine of the angle between these two vectors). Where this exceeds some threshold (0.9 would allow a range of 25 degrees) we allow accumulation and elsewhere only ablation. Figure 2 shows the distribution of net mass balance for the Tharsis Montes under these circumstances before the ice sheet has formed.

As the ice sheet grows the elevation- and orientation-dependent mass balance parameterization will respond to the changing ice sheet configuration. Fig. 3 shows ice thickness and surface elevations after 2.6 million years of growth. This is not an equilibrium configuration as the ice sheet is still growing. For comparison, Fig. 4 shows the glacial deposits.

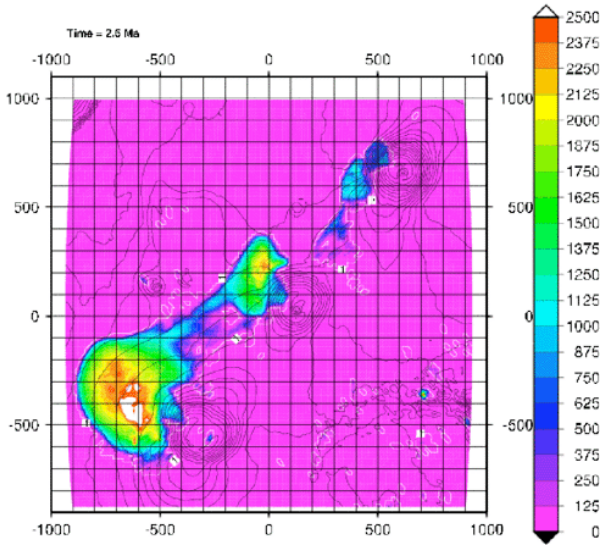

Figure 3. Surface thickness.

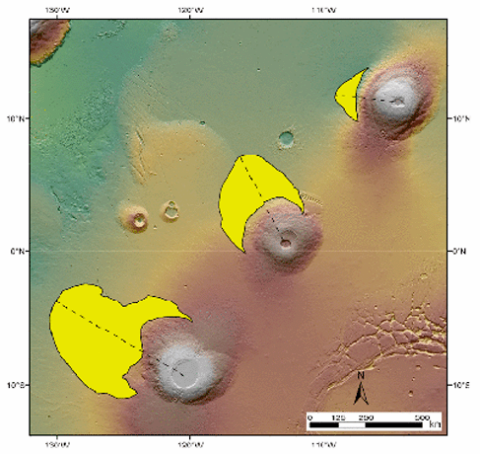

Figure 4. Glacial deposits [1,2].

Note the good agreement with the extensive Arsia Mons deposits. Also note that the presence of a slight topographic rise northwest of Pavonis Mons deflects the flow in a slightly more northward direction. Even the smaller Ascraeus Mons deposits are well represented.

Volumes and Areas: After 2.6 million years the combined volume of the ice sheets is 0.53 X 10^6 km^3. For comparison the North Polar Cap of Mars is thought to have a volume of approximately 1.5 X 10^6 km^3 [14]. The areal extent of the ice sheet is 0.51 X 10^6 km^2, approximately half the size of the present North Polar Cap. Interestingly the average thickness is ~1.02 km, very close to the estimated average thickness of the North Polar Cap (~1.03 km). A plausible mechanism would be to transport a significant portion of the NPC to the equatorial regions and deposit it on the flanks of Tharsis Montes.

Conclusions: 1) The properties of the martian atmosphere make the formation, accumulation, and behavior of snow and ice different from those on the Earth in significant ways (Fig. 1). 2) Using these guidelines, models of mass balance and spatial distribution on the western flanks of Tharsis Montes lead to patterns that are strikingly similar to the geological evidence for ice accumulation and glacial flow (Fig. 2, 3). 3) Areal and volumetric considerations predict accumulations that are consistent with the geologic evidence for the Tharsis Montes fan-shaped deposits; these volumes are comparable to about half the volume of the current North Polar Cap, implying that during periods of very high obliquity, a significant percentage of the polar cap is transported to the tropics. 4) Further refinements of these models will permit chronologies to be compared between predictions from obliquity cycle calculations [7] and the geologic record [1,2].

References: [1] J. Head and D. Marchant, Geology, 31, 641--644, 2003. [2] D. Shean, J. Head, and D. Marchant, JGR-P, in press, 2005. [3] D. Scott and J. Zimbelman, Map I-2480, USGS Misc. Invest. Ser., 1995. [4] J. Zimbelman and K. Edgett, Lunar Planet. Sci., 22, 31-44, 1992. [5] J. Fastook et al, LPSC 35, #1452, 2004. [6] D. Shean et al., LPSC 35, #1428, 2004. [7] J. Laskar et al., Icarus, 170, 343-364, 2004. [8] J. Head et al., Nature, 426, 797-802, 2003. [9] J.Glen, Proc. Royal Soc. London, 228, 519-538, 1955. [10] J. Fastook and M. Prentice. J. Glaciology, 40, 167--175, 1994. [11] P.Huybrechts et al., Ann. Glaciology, 23, 1-12, 1996. [12] A. Ingersoll, Science, 168, 972-973, 1970. [13] A. Pathare and D. Paige, Icarus, 2004. [14] M. Zuber et al., Science, 282, 2053-2060, 1998. [15] J. Benson et al., Icarus, 165, 34-52, 2003. [16] R. Haberle et al., LPSC 35, #1711, 2004. [17] M. Mischna et al., LPSC 35, #1861, 2004. [18] R. Elphic et al., LPSC 35, #2011, 2004.

VISCOUS FLOWS FROM POLEWARD-FACING WALLS OF IMPACT CRATERS IN MIDDLE LATITUDES OF THE ALBA PATERA AREA. T. Ishii[1], H. Miyamoto[2] and S. Sasaki[1, 3], [1]Department of Earth and Planetary Science, University of Tokyo, (te-tsu@eps.s.u-tokyo.ac.jp), [2]Department of Geosystem Engineering, University of Tokyo, [3]National Astronomical Observatory of Japan.

Introduction: A statistical analysis of the Mars Orbiter Laser Altimeter (MOLA) data shows that steep slopes (>20°) are less abundant in poleward-facing slopes than equatorward-facing slopes in middle latitudes in the both hemisphere [1]. The preferential flattening of poleward-facing slopes might be explained by melting of near-surface ground ice which is expected only on poleward-facing slopes in middle latitudes during periods of high obliquity [1]. This is consistent with the fact that recent Martian gullies associated with fluid flows are also frequently observed on poleward-facing slopes in middle latitudes [2], since gully formations might have played certain roles in the slope flattening processes. However, whether or not the near-surface melting of snow and/or ground ice happens at geologically recent times includes complicated problems; for example, it would also depend on the amount of trapped CO_2 on the open reservoirs such as the regolith at high latitude and the south residual polar cap [3]. In middle latitudes, tongue-shaped ridges (morphologically similar to terrestrial protalus ramparts or terminal moraines) are also dominantly observed at the base of poleward-facing walls of some impact craters [4]. It is suggested that tongue-shaped ridges would have some relation with viscous flows of ice-rich deposits [5, 6]. In this study, we identify whether the preferential slope flattening of poleward-facing slopes had or have continued through Amazonian, because it is generally considered that erosion rates on Mars would rapidly drop at the end of Noachian. We also discuss the formation of the north-south asymmetry of steep slopes on the basis of observations of MOC images and MOLA topographic profiles.

Methods: We study 77 impact craters in the Alba Patera area (25° N-60° N, 90° W-120° W) whose diameters are greater than 7 km. Since the most part of the Alba Patera area had been resurfaced during the periods from late Hesperian to early Amazonian [7], impact craters in the Alba Patera area would have formed after this period. Using the MOLA track data, we measure the maximum inclinations of both poleward-facing and equatorward-facing inner walls for each investigated impact craters. The maximum inclinations are measured for one MOLA shot spacing (about 0.3 km) and averaged in 3-5 MOLA tracks which pass near the center of impact craters.

Results: As shown in Figure 1a and 1b, the maximum inclinations of poleward-facing walls are generally smaller than those of equatorward-facing walls from around 30° N to 55° N, which is consistent with the previous statistical analysis (see Figure 5 in [1]). Inclinations of equatorward-facing walls below 45° N keep relatively high values of around 30°, which might reflect the angle of repose on Mars, and gradually decline with the increase of latitude (Figure 1a). On the other hand, inclinations of poleward-facing walls begin to decrease from 35° N (Figure 1a). In particular, an impact crater at 29.6° N shows an extraordinary low inclination of 20.6° (Figure 1a). These results indicate that the preferential flattening of poleward-facing slopes had occurred though Amazonian and might still continue today.

Figure 1c shows relative degrees of crater degradations. The degradation degree is defined as $R = (H - h)/H$, where H is initial crater depth which is altitudinal difference between the average rim height and the depth of the lowest point of crater floor, and h is actual crater depth [8]. H is calculated from an empirical equation for the aspect ratios (diameter:depth) of complex craters assembled by [9]. Most craters below 40° N have R-values of under 0.4, although R-values of most craters above 50° N are more than 0.4. The positive correlation between the R-value and the latitude may indicate preferential crater degradations in the higher latitudes.

Crater flattening by viscous flows of ice-rich materials: The processes involved in crater degradations would include dry mass wasting, fluvial incision and deposition, glacial and periglacial activities, lava filling, and dust and volcanic ash deposition. However, the systematical flattening of poleward-facing slopes in middle latitudes is difficult to be explained by most of these processes. Here we propose that slope flattening would be strongly influenced by stability of near-surface volatiles, that are ultimately controlled by solar insolation. Figure 2 shows a fresh crater with tongue-shaped deposits at the base of the poleward-facing (north-facing) wall. Tongue-shaped deposits are considered to have formed by viscous flows of ice-rich materials and contributed to crater degradations in middle latitudes [6]. We also consider that viscous flows of ice-rich materials from poleward-facing walls would mostly dominate flattening of craters, because almost all of degraded craters in middle latitudes in the Alba Patera area display flat floors, which are slightly inclined toward poleward (Figure 3, 4). We consider that floors of fresh craters such as Figure 2 might have been gradually filled by viscous flows of ice-rich materials to form flattened floors as shown in Figure 3. With the further progress of crater degradations, impact craters might be changed into almost flat, even floors such as Figure 4. Inclinations shown figure 4c suggest that viscous flows may be able to transport materials even under extremely low gradients of slope (<1°). As such, the preferential flattening of poleward-facing slopes can be formed by filling of crater cavities and/or erosions of rims by viscous flows of ice-rich materials which dominantly occur on poleward-facing walls in middle latitudes.

"Cold trap effect" of a CO_2 ice covering on poleward-facing slopes: In the above, we discuss the possibility of the repeated fillings of ice-rich materials for the crater flattening. Here we discuss how an ice-rich layer is formed only on poleward-facing slopes. We pay attention to a CO_2 ice covering which keeps ground surface temperature much below condensation point of water. Slope orientation would strongly affect near-surface CO_2 frost stability, and cold poleward-facing slopes would be covered with CO_2 ice for longer periods than other orientation [10]. If the surrounding atmosphere contains some moisture, CO_2 ice would continue to absorb the moisture, as if water vapor condenses on cold windows in a room during winter season. The "cold trap effect" of a CO_2 ice covering

might develop an ice-sheet and/or permafrost layer only on cold poleward-facing slopes in middle latitudes.

References: [1] Kreslavsky M. A. and Head J. W. (2003) *GRL, 30*, doi:10.1029/2003GL017795. [2] Malin M. C. and K. S. Edgett (2000) *Science, 288*, 2330–2335. [3] Haberle R. M. et al. (2003) *Icarus, 161*, 66-89, 2003. [4] Berman D. C. et al. (2004) *LPSC XXXV*, Abstract #1391. [5] Perron J. T. et al. (2003) *6th Mars Conf.*, Abstract #3236. [6] Berman D. C. et al. *Icarus*, in revision. [7] Scott D. H. and Tanaka K. L. (1986) USGS I-1802-A. [8] Forsberg-Taylor N. K. et al. (2004) *JGR, 109*, doi:10.1029/2004JE002242. [9] Garvin J. B. et al. (2003) *6th Mars Conf.*, Abstract #3277. [10] T. Ishii and S. Sasaki (2004) *LPSC XXXV*, Abstract #1556.

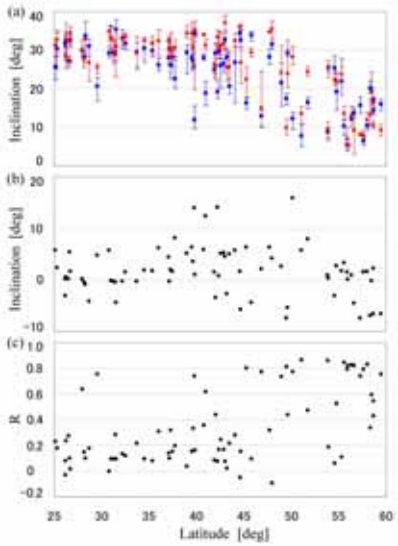

Figure 1: (a) The maximum inclinations of both equatorward-facing (red) and poleward-facing slopes (blue). Error bars show the upper or lower values of the maximum inclinations among 3-5 selected MOLA tracks. (b) Inclination differentials between equatorward-facing and poleward-facing slopes. (c) R-value.

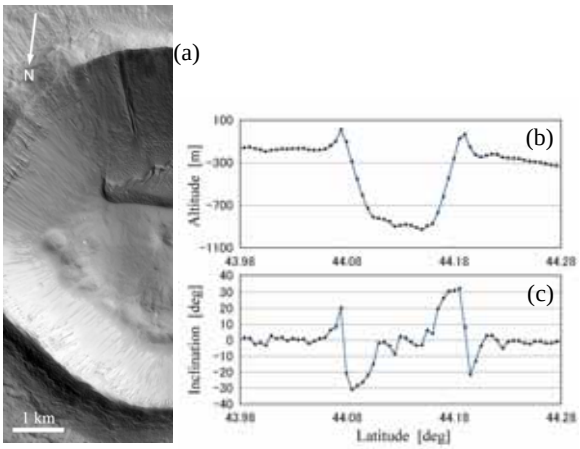

Figure 2: **(a)** A portion of MOC image R03-01123 near 44.1 °N, 91.1 °W (illuminated from the upper right). The diameter and R-value of the impact crater are about 6.95 km and 0.095, respectively. **(b)** Topographic profile of the crater shown in (a). **(c)** Inclinations between adjacent two MOLA shots. Positive value shows an equatorward-facing gradient and negative value shows a poleward gradient.

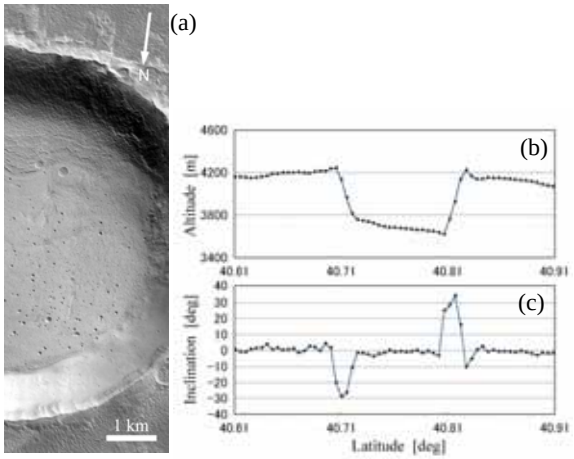

Figure 3: A portion of MOC image R15-02631 near 40.8 °N, 105.4 °W (illuminated from the upper right). The diameter and R-value of the impact crater are about 7.31 km and 0.36, respectively.

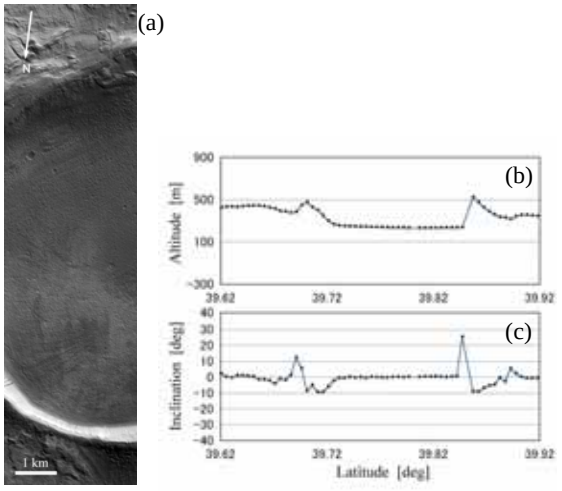

Figure 4: A portion of MOC image R09-01882 near 39.8 °N, 94.2 °W (illuminated from the upper right). The diameter and R-value of the impact crater are about 9.67 km and 0.74, respectively.

DEBRIS-COVERED GLACIERS WITHIN THE ARSIA MONS FAN-SHAPED DEPOSIT: IMPLICATIONS FOR GLACIATION, DEGLACIATION AND THE ORIGIN OF LINEATED VALLEY FILL. D. E. Shean[1], J. W. Head[1], and D. R. Marchant[2] [1]Brown University, Dept. of Geological Sciences, Providence, RI 02912 (David_Shean@Brown.edu), [2]Boston University, Dept. of Earth Sciences, Boston, MA 02215.

Introduction: Recent MOC and THEMIS data have shed new light upon intriguing flow-like features on Mars including viscous flow-like features [1], lobate debris aprons [2], concentric crater fill, lineated valley fill, and features interpreted as rock glaciers or debris-covered glaciers [3,4,5,6]. These features are distributed over low- to mid-latitudes and all appear to have experienced flow due to the presence of volatiles. Here we consider debris-covered glaciers – features that consist of a relatively pure glacier ice core covered by a thin (sub-m to m scale) layer of debris. A debris cover typically develops from rockfall or direct atmospheric dust deposition in the accumulation zone of the glacier and/or through sublimation of ice in the ablation zone, resulting in a surficial lag deposit of supraglacial and englacial debris. Using new data, we assess the origin of these features at Arsia Mons. We also consider how this interpretation may provide insight into processes of glaciation and deglaciation on Mars, and discuss its application to other areas containing candidate deposits of glacial origin.

Arsia Mons Smooth Facies: The Arsia Mons shield volcano has an 180,000-km^2 fan-shaped deposit present on its west-northwestern flank (Fig. 1). Our previous work suggests that this fan-shaped deposit represents the depositional remains of a large cold-based glacier that formed on the west-northwestern flank in the late Amazonian [5, 9]. One of the three main facies (smooth facies; Fig. 1) was interpreted as debris-covered rock glaciers [5]. These features consist of 20 to 100-km-long, broad, lobate plains, hundreds of meters thick with concentric ridges near the margins [5].

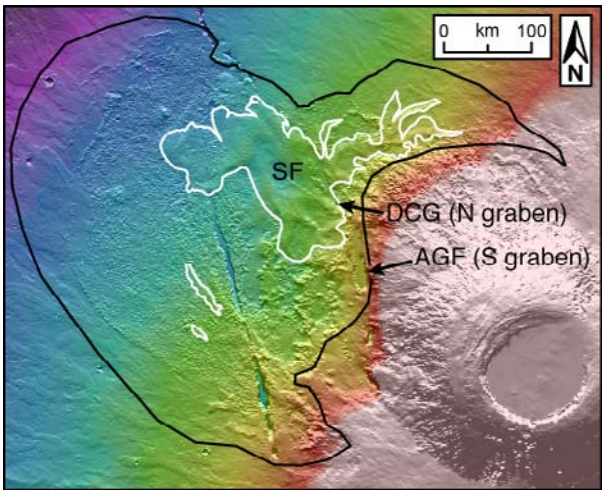

Figure 1: Arsia Mons fan-shaped deposit (black line) and smooth facies (SF, white line). The debris-covered glacier (Fig. 3) is labeled DCG and graben with arcuate graben fill (Fig. 4) is labeled AGF.

Similar features are well documented in the cold, hyperarid climate of the Dry Valleys in Antarctica [5,7,8]. Mullins Valley (Fig. 2) is of particular interest because it is occupied by a >5 km long, ~1 km wide, debris-covered glacier very similar in scale and morphology to those on Mars. As is characteristic of most debris-covered glaciers, Mullins displays a concentric ridged pattern. The debris cover (sublimation till) on Mullins (cm to <1 m thick) serves to insulate the underlying ice from the atmosphere, reducing sublimation to extremely low rates [10].

Recent THEMIS VIS images show some intriguing smaller-scale features near the eastern margins of the smooth facies at Arsia (Fig. 1). A distinctive flow-like feature (Fig. 3; ~12-15 km long, 2-4 km wide; >150-200 m thick in places) occupies a graben and does not have a "deflated" appearance like many flow-like features on Mars. In plan view, it consists of a proximal, steep-sided thinner section with marginal ridges that suggest previous occupation of a larger part of the valley. MOC data show a chevron-like pattern of lineations similar to terrestrial glaciers. To the NW, it expands into a wider, lobate series of concentric ridges (compare Figs. 2 and 3) and appears to fill depressions in previous topography (Fig. 3). We interpret this flow-like feature as a debris-covered glacier that may still contain a significant ice core and may represent the most recent phase of glaciation at Arsia. The marginal depressions suggest that the ice-rich upper part of the glacier may have been 'beheaded' during interglacials, followed by the formation of a new lobe when glacial conditions return.

An 8 to 15-km-wide graben cuts through the center of the Arsia fan-shaped deposit (Fig. 1, 4). This graben contains arcuate fill material that appears to originate at two cirque-like alcoves along the base of the scarp in the SE corner with concentric ridges indicating northward flow within the graben. Although the valley floor currently lies below the graben rim, the lobate and ridged deposits on the graben rim indicate that at one time, debris-covered flowing ice completely filled the graben, breached the walls, and extended an additional 5-8 km to the east and west of the graben (Fig. 4). Subsequent deglaciation then caused the down-wasting of the ice to produce the current topography; the material still appears to be a few hundred meters thick and is characterized by many concentric ridges suggesting substantial flow. On the basis of topography, the remaining material still appears to be ice-cored.

Discussion and Summary: 1) Debris-covered glaciers are valuable morphological indicators of climate change on Earth and Mars. 2) We interpret these features in the smooth facies at Arsia to represent the latest phases of glacial activity associated with the fan-shaped deposit. 3) These data also provide insight into both glaciation and deglaciation processes here and elsewhere on Mars, showing examples of advance (Fig. 3), overflowing of valley margins (Fig. 4), retreat during deglaciation (decapitation, Fig. 3; down-wasting, Fig. 4), and readvance (Fig. 3). 4) The elongate graben (Fig. 4) shows abundant evidence of being filled with debris-covered ice, overflowing the margins, and then retreating during deglaciation. This provides an excellent analog for the nature of lineated valley fill (LVF) [11], and a) how it can form on portions of valley interiors and flow along the long axis of the valley, b) how it can fill valleys and overflow onto the valley margins [12], and c) how LVF can form in closed valleys of limited areal extent.

References: [1] Milliken R.E. et al. (2003) *JGR, 108(E6)*, 5057. [2] Mangold N. (2003) *JGR, 108(E4)*, 8021. [3] Head J.W. et al. (2005) *Nature*, in press. [4] Neukum G. et al. (2004) *Nature, 432*, 971-979. [5] Head J.W. & Marchant D.R. (2003) *Geology, 31*, 641-

644. [6] Milkovich S.M. & Head J.W. (2003) *6th Mars*, #3149. [7] Rignot E. et al. (2002) *GRL, 29(12)*, 1607. [8] Hassinger J.M. & Mayewski P.A. (1983) *Arctic & Alpine Res., 15(3)*, 351-358. [9] Shean D.E. et al. (2005) *JGR-P*, in press. [10] Marchant, D. R. et al., *GSAB*, 114, 718-730 (2002). [11] Head, J. W. et al., *LPSC 36*, #1208 (2005). [12] Head, J. W. et al., *LPSC 36* (2005).

Figure 2: Aerial photograph of Mullins valley debris-covered glacier, Antarctica. Note the distinctive concentric ridges.

Figure 3: THEMIS VIS mosaic of flow-like feature within northern graben, interpreted as a debris-covered glacier.

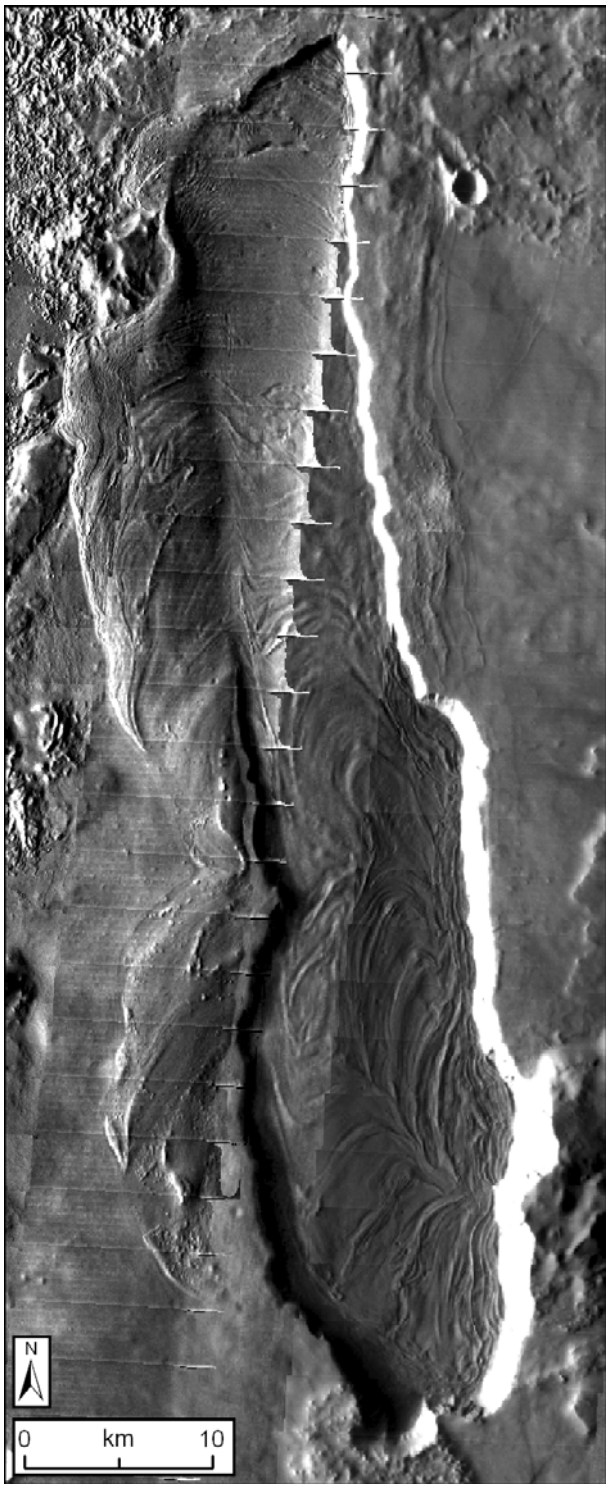

Figure 4: THEMIS VIS and IR mosaic of arcuate fill material in southern graben at Arsia. Note the material to the west and east of the graben walls and the concentric ridges that appear to originate at the two cirque-like alcoves on the southeastern wall.

CENTRAL MOUNDS IN MARTIAN IMPACT CRATERS: ASSESSMENT AS POSSIBLE PERENNIAL PERMAFROST MOUNDS (PINGOS). S. E. H. Sakimoto[1], [1]Department of Civil Engineering and Geological Sciences, 156 Fitzpatrick Hall, University of Notre Dame, Notre Dame, IN, 46556, Email: ssakimot@nd.edu.

Introduction: Impact craters on Mars are a window into the martian surface and near-surface revealing local target properties as well as local geologic processes. The central peaks or mounds of martian impact craters are key indicators in determining these target properties and processes. Here, we show some of the range of non-typical crater central peaks and consider post-impact formation and modification origins for some or all of their topographic signature, with particular emphasis on pingo-like (perennial permafrost mound) modes of origin.

Data and approach: The typical central peak topography for martian impact craters has been well-defined (e.g. [1]), and some anomalies have since been studied as having probable post-impact major modifications, such as the layered stratigraphy in Gale crater [2], (see Figure 1), the broad central mounds of the north polar impact craters (e.g. [3], Figure 2 and Figure 3), and the pitted cones in the south polar region near Malea Planum (see Figure 4).

Recent work in the equatorial region of Mars has suggested that there is evidence for pingo-like or small perennial permafrost mounds in the Athabascan, Valles region [4,5] that may be tapping sources of water related to the proposed late Amazonian floods in the region (e.g. [6]). While these equatorial features are small (tens of meters), the globally mapped near-surface ground ice abundance [7,8] is also very low. These small features mapped by Burr et al., [4,5] are within fluvial channels, rather than impact craters. While the equatorial impact craters might have a larger potential groundwater or permafrost budget than the equatorial channels, the central mounds of impact craters in the equatorial regions generally show more apparent evidence of sedimentary filling and exhumation than of possible permafrost processes. For example, Gale crater [2, 9] and Figure 1, shows ample evidence of probable sedimentary stratigraphy [2, and others], and central peak rising above the rim elevations, and is superposed on the dichotomy boundary [9]. We are therefore considering polar impact craters for permafrost processes and pingo formation. The polar impact craters have profoundly different styles of central mounds than any other regions on Mars [3]. In the north polar region, these mounds occupy a large fraction of the crater floor, are roughly concentric to the crater center with a usual shallower southern exposure (inverted in the south polar region) that suggests a significant volatile component lost through solar-driven sublimation (see figures 2 and 3). Several of the most pole-ward examples retain bright frost cover throughout local summer seasons, but regardless of such apparent surface frost, the topographic signature for polar region craters frequently includes these gentle central mounds, which are frequently difficult to detect in images due to their subdued topography and probable dust cover [3]. While these craters are clearly potential cold-traps for retaining frost and dust and thus accumulating layered central polar-like deposits, we suggest that these central mounds have a possible alternate origin as pingo-like features. In support of this, we have the overall mound-like shape, with a concentric low that is difficult to model with solely sedimentary accumulations, the generally systematic equator/poleward slope differences, with the mound slope facing the poles steeper than the equatorial slopes (suggesting possible uneven volatile losses). On earth, pingos come in hydrostatic (closed system pingos generally found in flat terrains with continuous permafrost) and hydraulic (open system pingos found in local basins or valleys) varieties. On Mars, the impact crater topography may well provide the hydraulic head and permafrost disruption (initial or topographic) to initiate pingo formation and growth. Long periods of permafrost action not generally available on Earth could explain their growth to such large sizes (an order of magnitude or more larger than terrestrial varieties). Pingo collapse can form summit pits within the mounds, as seen in the possible equatorial features discussed by Burr et al. [4,5]. There are at least several polar impact craters with pronounced central mound features with collapse pits, which were previously suggested as potential volcanic features (see figure 4). These may have alternate possible origins as perennial ground ice features. This study presents topographic characterization and modeling of several dozen polar impact crater central deposits as potential pingo features. And compares the scaling, possible growth times, and morphology to terrestrial features.

References: [1] Garvin et al., 2003, 6th International Conference on Mars, Abstract # 3277, [2] Edgett and Malin, LPSC Abstract # 1005, 2001, [3] Garvin et al., ICARUS, vol 144, pp329-352,

2001, [4] Burr, D.M. et al., AGU Abstract P13A-0982, 04AGUFM.P13A0982B, 2004, [5] Burr, D.M. et al., ICARUS, In Press, 2005. [6] Burr D.M., et al., GRL, Vol 29, pp.13-1, CiteID 1013,DOI 10.1029/2001GL013345 [7] Boynton et al., 2002, Science 296, 81-85, [8] Feldman et al., 2002, Science 297, 75-78, [9] Frey et al., 1998, LPSC Abstract #1507 [10] Gurney, 1998, Progress in Physical Geography, 22, 307-324.

Acknowledgements: I thank Devon Burr, James Garvin and Herb Frey for helpful discussions on central crater mounds. Early portions of this cratering work were supported by the MOLA Science Team.

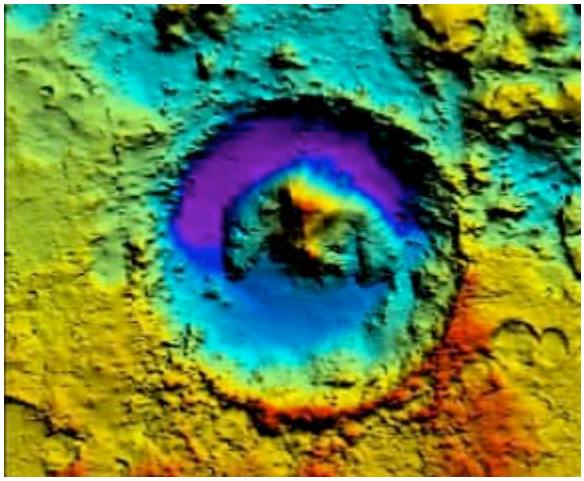

Figure 1. MOLA topography for the 155 km diameter Gale crater near 6S, 138E. The central mound rises nearly 5 km above the lowest floor regions, lies above much of the the rim, and shows clear signs of layering [ ].

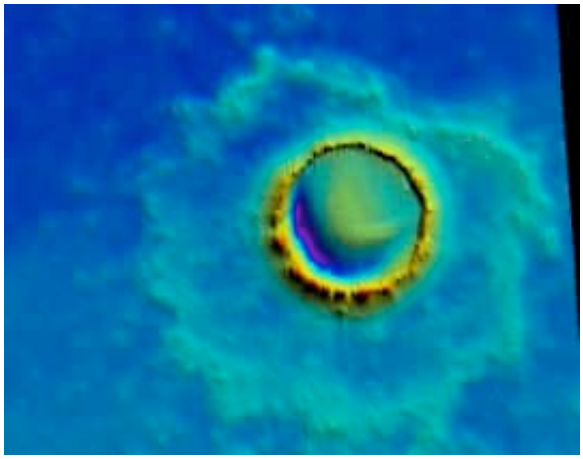

Figure 2 MOLA topography for a north polar region crater approximately 30 km in diameter near 77N, 90E with an asymmetric central mound 500 m high. Note that central mound is ringed by a concentric depression.

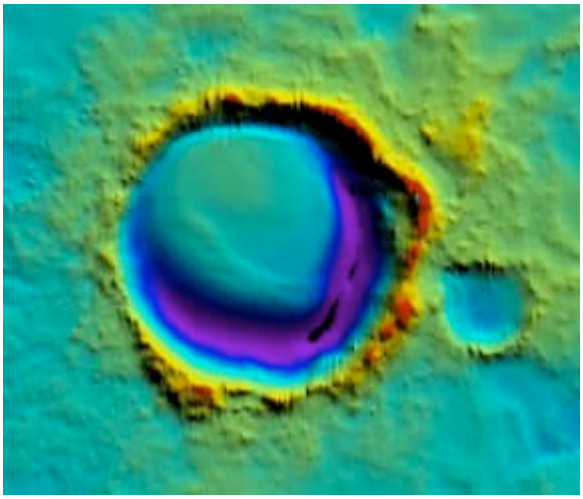

Figure 3. MOLA topography for a north polar region crater near 77N, 215E approximately 55 km in diameter with a asymmetric central mound filling much of the crater floor. Note that central mound rises 1.4 km above lowest current floor elevations, and is ringed by a concentric depression.

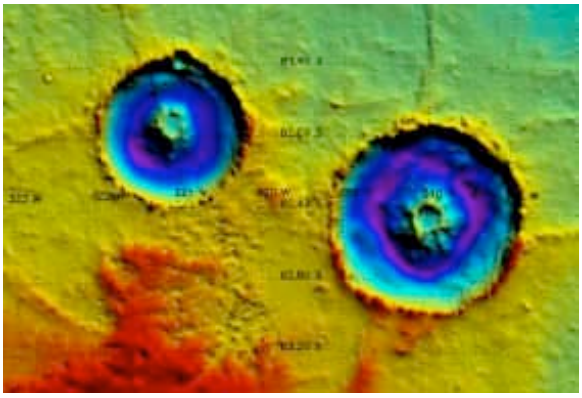

Figure 4. MOLA topography for two south polar region craters near 62S, 40E with central mounds with summit depressions. The left and right impact craters are approximately 50 km, and 65 km in diameter, respectively, with central mounds up to 1.1 km high.